TECHNICAL REPORT STANDARD TITLE PAGE

1. Report No.	2. Government Accession No.	3. Recipient's Catalog No.
FHWA/TX-81/20+242-2		

4. Title and Subtitle	5. Report Date
THE INFLUENCE OF SHEAR ON LAPPED SPLICES IN REINFORCED CONCRETE	July 1981
	6. Performing Organization Code
7. Author(s)	8. Performing Organization Report No.
A. J. Zekany, S. Neumann, J. O. Jirsa, and J. E. Breen	Research Report 242-2
9. Performing Organization Name and Address	10. Work Unit No.
Center for Transportation Research The University of Texas at Austin Austin, Texas 78712	11. Contract or Grant No. Research Study 3-5-78-242
	13. Type of Report and Period Covered
12. Sponsoring Agency Name and Address Texas State Department of Highways and Public Transportation; Transportation Planning Division P. O. Box 5051 Austin, Texas 78763	Interim
	14. Sponsoring Agency Code

15. Supplementary Notes

Study conducted in cooperation with the U. S. Department of Transportation Federal Highway Administration. Research Study Title: "Influence of Casting Position and of Shear on the Strength of Lapped Splices"

16. Abstract

The primary objective of this investigation was to study the effects of level of shear, amount of transverse reinforcement, and casting position on the strength of lapped splices. A limited number of tests were conducted to examine the influence of concrete strength, slump, and bar size on splice performance. In addition, an exploratory study is reported on the influence of high range water-reducing admixtures (superplasticizers) on splice performance.

Twelve beam specimens containing both top and bottom splices were constructed providing a total of twenty-four separate tests. Ten specimens contained four #11 bars (22 in. lap length) and two contained five #9 bars (16 in. lap length). The concrete varied from 4025 psi to 5700 psi. The parameters of cover, spacing, edge distance, and lap length for a given bar size were kept constant in each group. The behavior of the beam specimens was studied in terms of the crack patterns and steel strain distributions. The measured average bar stresses are compared to evaluate the effect of the variables.

The results provide additional data for evaluating design equations which have been recommended by ACI Committee 408 to change the ACI Building Code (ACI 318-77). The ACI Code is primarily intended for building design; however, AASHTO Code provisions closely follow the ACI Code and are applicable to bridges as well as other transportation structures.

17. Key Words	18. Distribution Statement
reinforced concrete, shear, beams, lapped splices, strength, slump, bar size, crack patterns, steel strain distributions	No restrictions. This document is available to the public through the National Technical Information Service, Springfield, Virginia 22161.

19. Security Classif. (of this report)	20. Security Classif. (of this page)	21. No. of Pages	22. Price
Unclassified	Unclassified	100	

Form DOT F 1700.7 (8-69)

THE INFLUENCE OF SHEAR ON LAPPED SPLICES IN REINFORCED CONCRETE

by

A. J. Zekany
S. Neumann
J. O. Jirsa
and
J. E. Breen

Research Report No. 242-2

Research Project No. 3-5-78-242

Influence of Casting Position and of Shear on the Strength of Lapped Splices

Conducted for

Texas
State Department of Highways and Public Transportation

In Cooperation with the
U. S. Department of Transportation
Federal Highway Administration

by

CENTER FOR TRANSPORTATION RESEARCH
BUREAU OF ENGINEERING RESEARCH
THE UNIVERSITY OF TEXAS AT AUSTIN

July 1981

The contents of this report reflect the views of the authors who are responsible for the facts and accuracy of the data presented herein. The contents do not necessarily reflect the views or policies of the Federal Highway Administration. This report does not constitute a standard, specification or regulation.

P R E F A C E

In this report, the second phase of a study on "The Influence of Casting Position and of Shear on Strength of Lapped Splices," is presented. The objective of the project was to review existing data and to conduct an experimental program for determining the effect of casting position and shear on anchorage strength and to suggest modification, if needed, for design codes. In this report the influence of shear on splices in reinforcing bars is described. In the first phase of the project the influence of casting position on development and splice length of reinforcing bars is described. In the final report, suggestions for changes in design specifications will be presented.

The work was sponsored by the Texas State Department of Highways and Public Transportation and the Federal Highway Administration and administered by the Center for Transportation Research at The University of Texas at Austin. Close liaison with the State Department of Highways and Public Transportation has been maintained through Mr. Melvin C. Jackson, James C. Wall, and Warren K. Sandberg, who served as contact representatives during the project, and with Mr. William Dallas of the Federal Highway Administration.

The project was conducted in the Phil M. Ferguson Structural Engineering Laboratory located at the Balcones Research Center of The University of Texas at Austin.

S U M M A R Y

The primary objective of this investigation was to study the effects of level of shear, amount of transverse reinforcement, and casting position on the strength of lapped splices. A limited number of tests were conducted to examine the influence of concrete strength, slump, and bar size on splice performance. In addition, an exploratory study is reported on the influence of high range water-reducing admixtures (superplasticizers) on splice performance.

Twelve beam specimens containing both top and bottom splices were constructed providing a total of twenty-four separate tests. Ten specimens contained four #11 bars (22 in. lap length) and two contained five #9 bars (16 in. lap length). The concrete varied from 4025 psi to 5700 psi. The parameters of cover, spacing, edge distance, and lap length for a given bar size were kept constant in each group. The behavior of the beam specimens was studied in terms of the crack patterns and steel strain distributions. The measured average bar stresses are compared to evaluate the effect of the variables.

The results provide additional data for evaluating design equations which have been recommended by ACI Committee 408 to change the ACI Building Code (ACI 318-77). The ACI Code is primarily intended for building design; however, AASHTO Code provisions closely follow the ACI Code and are applicable to bridges as well as other transportation structures.

I M P L E M E N T A T I O N

The results of this study will permit further refinement of recommendations resulting from Project 3-5-72-154. The recommendations included in that study have been the subject of considerable discussion in appropriate committees of the American Concrete Institute. The Committee on Bond and Development of Reinforcement (ACI 408) has made a recommendation to the Building Code Committee of the American Concrete Institute (ACI 318) for changes in the provisions for development length and splices. The proposed changes are based largely on the work carried out under Project 154. Because AASHTO provisions are based primarily on ACI design recommendations, it is likely that the changes in ACI 318 will eventually appear in AASHTO Specifications. To provide a design recommendation which handles all aspects of development and splice length of reinforcement, including the effect of casting position and shear, the research conducted under Project 242 will further improve design recommendations.

Current design specifications contain confusing, often anomalous, statements which are difficult for designers to apply in design situations. The implementation of the results from this program should help to clarify the role of casting position, shear, and properties of fresh concrete on the strength of anchored bars.

C O N T E N T S

Chapter		Page
1	INTRODUCTION	1
	1.1 General	1
	1.2 Objective and Scope	2
2	A REVIEW OF THE STRENGTH AND BEHAVIOR OF LAPPED SPLICES	5
	2.1 Mechanics of Stress Transfer	5
	2.2 Splice Strength	9
	2.3 Effect of Moment Gradient	16
	2.4 Effect of Changes in Concrete Properties	16
	2.4.1 Slump	16
	2.4.2 Presence of High Water Reducing Admixtures	17
	2.5 Current ACI and AASHTO Code Provisions	18
3	EXPERIMENTAL PROGRAM	19
	3.1 Test Specimens	19
	3.2 Variables	19
	3.2.1 Level of Shear	19
	3.2.2 The Transverse Reinforcement	22
	3.2.3 Casting Position	22
	3.2.4 Concrete Strength	22
	3.2.5 Concrete Consistency	23
	3.2.6 Bar Size	23
	3.2.7 Splice Location	23
	3.3 Specimen Geometry	24
	3.4 Materials	24
	3.4.1 Concrete	24
	3.4.2 Reinforcing Steel	28
	3.5 Instrumentation	28
	3.6 Fabrication	28
	3.7 Formwork and Casting Procedure	30
	3.8 Test Frame and Loading System	32
	3.9 Testing Procedure	32
	3.10 Data Reduction	36
4	SPLICE BEHAVIOR AND TEST RESULTS	39
	4.1 Introduction	39

Chapter Page

4.2 Crack Patterns 39
4.2.1 40 Inch Shear Span 44
4.2.2 53 Inch Shear Span 44
4.2.3 80 Inch Shear Span 49
4.3 Strains in the Longitudinal Reinforcement 51
4.3.1 Steel Strains Across the Splices 54
4.3.2 Steel Strains Along the Splice 57
4.3.3 Strains in the Transverse Reinforcement . 57
4.3.4 Strains at Selected Points Around Transverse Reinforcement 65

5 EVALUATION OF TEST RESULTS 69

5.1 Introduction 69
5.2 Level of Shear 69
5.3 Transverse Reinforcement 71
5.4 Configuration of Transverse Reinforcement 74
5.5 Casting Position 74
5.6 Concrete Strength 75
5.7 Slump 75
5.8 Splice Location 78

6 SUMMARY AND CONCLUSIONS 83

6.1 Summary 83
6.1.1 Test Program 83
6.1.2 Variables 83
6.1.3 Specimen Behavior 84
6.2 Conclusions 85
6.2.1 Effect of Test Variables 85

REFERENCES 87

F I G U R E S

Figure		Page
2.1	Calculation of bond stresses, u	6
2.2	Forces between deformed bar and concrete	8
2.3	Internal cracks surrounding a deformed bar in concrete	10
2.4	Failure patterns of deformed bars	11
2.5	Failure patterns in lapped splices	12
2.6	Definition of transverse reinforcement, A_{tr}	15
3.1	Side view of test specimen (load shown for top cast splice test)	20
3.2	Specimen with splice offset a distance d from support	25
3.3	Cross section of specimens	26
3.4	Stress-strain relationship for reinforcing steel	29
3.5	Reinforcement	31
3.6	Loading diagrams	33
3.7	Side view of testing frame (top splice test)	34
3.8	End view of testing frame with rams	35
3.9	Test frame with a specimen in place	36
3.10	Adjustment for dead load strains	38
4.1	Crack patterns, Test #5	40
4.2	Modes of splitting failure	42
4.3	Tension face splitting--one edge only	43
4.4	Crack patterns, 40 in. shear span, #11 bars, $f'_c \approx 4$ ksi	45

Figure | Page

4.5 Crack patterns, 40 in. shear span, #11 bars, $f'_c \approx 5$ ksi 46

4.6 Crack patterns, 53 in. shear span, #11 bars, $f'_c \approx 4$ ksi 47

4.7 Crack patterns, 53 in. shear span, #9 bars, $f'_c \approx 6$ ksi 48

4.8 Crack patterns, 80 in. shear span, #11 bars, $f'_c \approx 4$ ksi 50

4.9 Load vs. strain, Test #4, 53 in. shear span 52

4.10 Load vs. strain, Test 20, 40 in. shear span 55

4.11 Steel strain distribution across the end of the splice, Test 24 56

4.12 Steel strain distribution across the end of the splice, Test 11 58

4.13 Steel strain history along the splice, Test 22, 53 in. shear span, no transverse reinforcement 59

4.14 Steel strains along the splice, Test 11, 40 in. shear span, four 6mm @ 5 in. 60

4.15 Load vs. strain in stirrups, Test 14, bottom cast, 53 in. shear span 61

4.16 Load vs. strain in stirrups, Test 23, bottom cast, 53 in. shear span 62

4.17 Load vs. strain in stirrups, Test 12, bottom cast, 40 in. shear span 63

4.18 Load vs. strain in stirrups, Test 5, bottom cast, 53 in. shear span 64

4.19 Strains around the transverse reinforcement, Test 20, top cast, #11 bars, 40 in. shear span 66

4.20 Strains around the transverse reinforcement, Test 1, top cast, #11 bars, 40 in. shear span 68

5.1 Variation in bond strength with concrete compressive strength 77

Figure Page

5.2a Freebody diagram of concrete block between maximum flexural crack and shear crack 79

5.2b Moment diagram at section A for tests compared 79

TABLES

Table		Page
3.1	Details of Test Specimens	21
3.2	Concrete Properties	27
3.3	Load Adjustment due to Dead Load Moment	37
4.1	Summary of Steel Strains at Failure	53
5.1	Summary of Test Results	70
5.2	Effect of Level of Shear on the Splice Strength . . .	72
5.3	Effect of the Amount of Transverse Reinforcement on the Splice Strength	73
5.4	Effect of the Configuration of Transverse Reinforcement on Splice Strength	73
5.5	Effect of Slump on Corresponding Bottom and Top Tests for Beam Specimens with the Same Characteristics . . .	76
5.6	Effect of Slump on Bottom and Top Tests for the Same Beam Specimen	76
5.7	Effect of Splice Location on Splice Strength	80

CHAPTER 1

INTRODUCTION

1.1 General

The interaction between steel and concrete, i.e. bond and development of reinforcement is always of concern to engineers designing reinforced concrete structures. Limitations on the length of bars for fabrication, economic considerations, and continuation of a trend toward the design and construction of larger structures require that large numbers of reinforcing bars be spliced. For splices, the interaction becomes especially critical. While many types of mechanical splices are available, the lapped splice is used most frequently. With the use of larger bar sizes and higher strength steels, the amount of force which must be transferred from bar to bar is increased substantially. Because a splice failure often involves splitting of the concrete, the failure can be sudden and spectacular. A splice failure usually results in a separation of the concrete cover surrounding the bar. To ensure a ductile failure, adequate embedment length, concrete cover, clear spacing between bars, and transverse reinforcement must be provided.

In a recent study by Orangun, Jirsa, and Breen [1] the test data from many investigations was reevaluated resulting in the formulation of a design equation for the required lap length to develop yield in the reinforcement. The design equation incorporates variables which are not taken into account in current provisions [5,16] but which influence bond behavior. These variables include cover, spacing between bars, and transverse reinforcement in addition to the variables in current design codes: yield point, concrete strength, and bar size.

Extensive review of the literature on splice tests shows that most of these tests were conducted on bottom cast, horizontal splices subjected to constant moment over the splice length. Very few tests are reported regarding the influence of the following variables on the performance of

lapped splices: (1) bar position during casting (bottom or top cast, horizontal or vertical orientation), (2) severe shear or moment gradient, and (3) concrete consistency (changes in slump produced by admixtures or mix proportions). Studies of the effect of casting position [2,3,4] conducted as part of this overall project have shown that the reduction of bond strength was a function of the amount of concrete cast below the bar. Other studies [5] have indicated that high shear on the section combined with high tensile stresses may lead to a reduction in anchorage strength of lapped splices. There has been speculation that transverse reinforcement stressed highly by shear may not be effective in resisting splitting due to anchorage (bond) forces and vice versa.

The study reported herein is part of a larger research program to determine the influence of casting position and shear (or moment gradient) on the strength of anchored bars and lapped splices. In the first phase [4], the influence of casting position and bar orientation on the development of deformed bars and on the strength of lapped splices was studied. In the second phase, reported herein, lapped splices in beams subjected to shear were studied. The variables include level of shear, transverse reinforcement, changes in concrete strength or slump (as influenced by water content or by high range water reducing admixtures), and bar sizes.

1.2 Objective and Scope

The primary objective of this investigation was to study the effects of level of shear, amount of transverse reinforcement and casting position on the strength of lapped splices. A limited number of tests were conducted to examine the influence of concrete strength, slump, and bar size on splice performance. In addition an exploratory study is reported on the influence of high range water reducing admixtures (superplasticizers) on splice performance.

Twelve beam specimens containing both top and bottom splices were constructed providing a total of twenty-four separate tests. Ten specimens contained four #11 bars (22 in. lap length) and two contained five #9 bars (16 in. lap length). The concrete strength varied from 4025 psi to 5700 psi. The parameters of cover, spacing, edge distance, bar diameter

(#9 and #11), and lap length for a given bar size were kept constant in each group.

The behavior of the beam specimens is discussed in terms of the crack patterns and steel strain distributions. The measured average bar stresses are compared to evaluate the effect of the variables.

The results provide additional data for evaluating the design equation proposed by Orangun, et al. [1], which forms the basis for changes to the ACI Building Code (ACI 318-77) [6] recommended by ACI Committee 408 [7]. The ACI Code is primarily intended for building design; however, AASHTO Code [8] provisions closely follow the ACI Code and are applicable to bridges as well as other transportation structures.

CHAPTER 2

A REVIEW OF THE STRENGTH AND BEHAVIOR OF LAPPED SPLICES

2.1 Mechanics of Stress Transfer

The transfer of stress between reinforcing steel and concrete is expressed using the concept of bond stress for the mechanics of transferring of the tension force in the bars to the adjacent concrete. Bond stresses are assumed to represent an average shearing stress acting on the surface of the bar along the length of the splice. The equilibrium of a short length of a bar (Fig. 2.1) in a beam section subjected to a moment gradient requires that:

$$\Delta T = \Sigma_o \cdot u \cdot dx \tag{2.1}$$

where ΔT is the change in the bar tensile force, Σ_o is the sum of the perimeters of the bars in tension, u is the average bond stress over dx, the length of the element under consideration.

The internal tension force T varies at the same rate as the external bending moment M; therefore,

$$\Delta T = \frac{\Delta M}{jd} = \frac{Vdx}{jd} \tag{2.2}$$

where ΔM is the change in bending moment at the section considered, j is the ratio of the distance between the centroid of compression and the centroid of tension to the depth d, and V is the shear force at the section considered. Then combining Eqs. (2.1) and (2.2),

$$u = \frac{V}{\Sigma_o jd} \tag{2.3}$$

This equation indicates that when the rate of change of external bending moment (i.e., the shear force) is high, the flexural bond stress will also increase. However, Eq. (2.3) oversimplifies the situation because

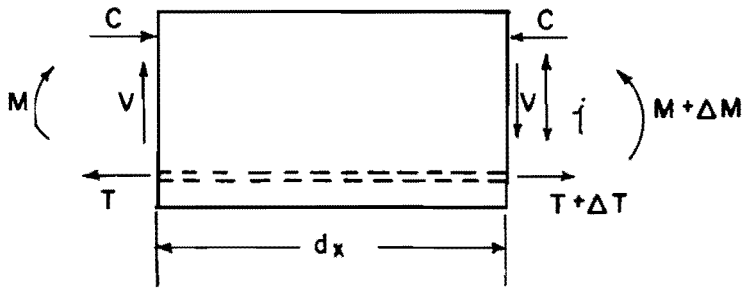

(a) FORCES ACTING ON SECTION OF BEAM WITH LENGTH d_x

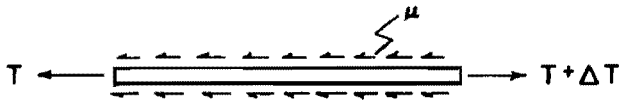

(b) FORCES ACTING ON EMBEDDED BAR

Fig. 2.1 Calculation of bond stresses, u

cracking in the concrete at discrete intervals along the member results in a redistribution of bond stresses.

Tests by Ferguson and Briceno [9] and also by Tepfers [10] showed that strain variations along the length of lapped splices become approximately linear near ultimate load. Therefore, equating the tensile force on the bar with the total bond force on the surface area of the bar results in the following equation:

$$T = \frac{\pi d_b^2 f_s}{4} = \ell_s \pi d_b u \tag{2.4}$$

and rearranging,

$$u = \frac{f_s d_b}{4 \ell_s} \tag{2.5}$$

where T is the tension force in the bar, d_b the bar diameter, ℓ_s is the splice length, and f_s is the stress in the reinforcing bar.

When steel reinforcement consisted of plain bars without lug deformations, bond was thought of as the adhesion between concrete paste and the surface of the bar. Slippage of the bar at low tensile stress in the reinforcement was sufficient to break the adhesion, leaving only friction to resist bar movement relative to the adjacent concrete. Typically, plain bars failed by longitudinal splitting if the adhesion and friction resistance were high enough, or by pullout failure leaving a round hole when adhesion and friction were low [8].

Deformed bars were designed to change the behavior with less reliance on adhesion and friction and more on mechanical interlock through bearing of the lugs against the concrete. Bond failures with deformed bars almost always involve concrete splitting. The force exerted on the concrete by the lugs is inclined at an angle β to the axis of the bar as shown in Fig. 2.2. From measurements of internal cracks radiating from a tension bar embedded in concrete, Goto [9] found that the angle of inclination β varied from 45° to 80°, depending on the amount of crushed concrete

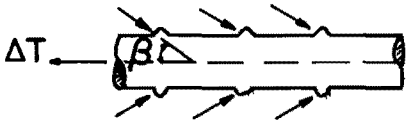

(a) Bond Force on Bar

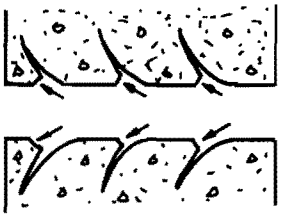

(b) Reaction on Concrete

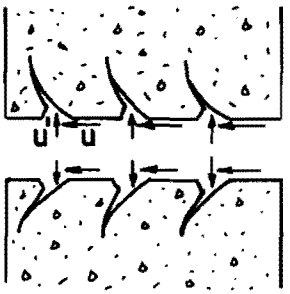

(c) Components on Concrete

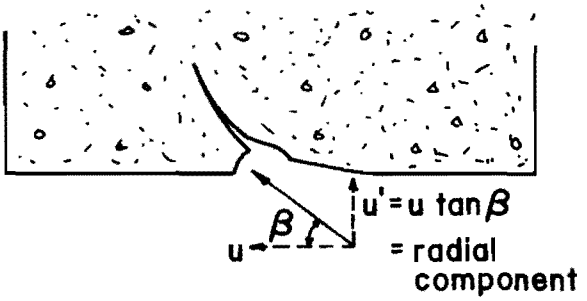

(d) Tangential and Radial Components

Fig. 2.2 Forces between deformed bar and concrete

in front of the lugs for various rib patterns on the reinforcement. The radial component causes splitting of the surrounding concrete at failure. Prior to splitting, radial stresses are balanced by tensile stresses in the concrete surrounding the bar. The radial stress can be considered as an internal pressure acting against a thick-walled cylinder (Fig. 2.3) having an inner diameter equal to the bar diameter d_b and a thickness C which is the smaller of (1) the clear bottom cover C_b, or (2) half the clear spacing C_s between the next adjacent bar (Fig. 2.4). Splitting cracks form when the tensile capacity of the concrete cylinder is reached.

The type of splitting failure is dependent on the values of C_b and C_s [1]. With $C_b > C_s$, a horizontal split develops at the level of the bars, and is termed a "side split failure." With $C_s > C_b$, longitudinal cracks through the bottom cover occur prior to splitting through the plane of the bars. Such a failure is termed a "face and side split failure." With $C_s \gg C_b$, a "V-notched failure" occurs with longitudinal cracking followed by inclined cracking. In a lapped splice where the bars are side by side, the two cylinders to be considered for each bar interact to form an oval ring as shown in Fig. 2.5. The failure patterns are similar to those of single bars. Splitting is the first sign of bond distress and progressive splitting is generally the cause of bond failure. Confinement of the longitudinal steel by transverse reinforcement may significantly delay a bond failure until several splitting cracks have formed.

2.2 Splice Strength

The radial component of the forces acting on the bars are dependent on the value of the angle β between the resultant force on the concrete and the axis of the bar. Because the value of β is dependent on the amount of crushed concrete in front of the lugs, a theoretical derivation of a splice length equation was impractical. Orangun, et al. [1] used an empirical method to develop an equation for the strength of lapped splices for deformed bars. By using a regression analysis of the results of a number of well-documented lapped splice tests, the following equation in

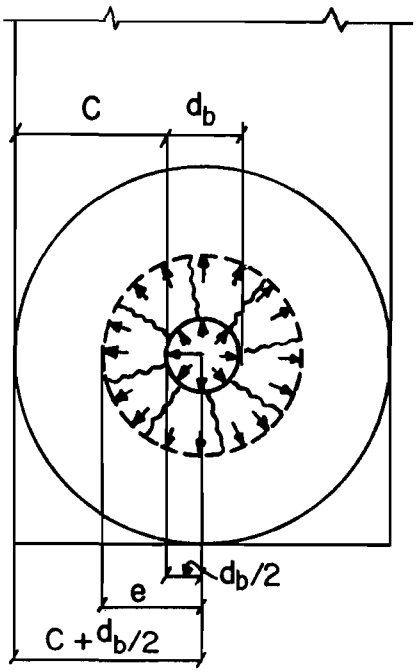

Fig. 2.3 Internal cracks surrounding a deformed bar in concrete.

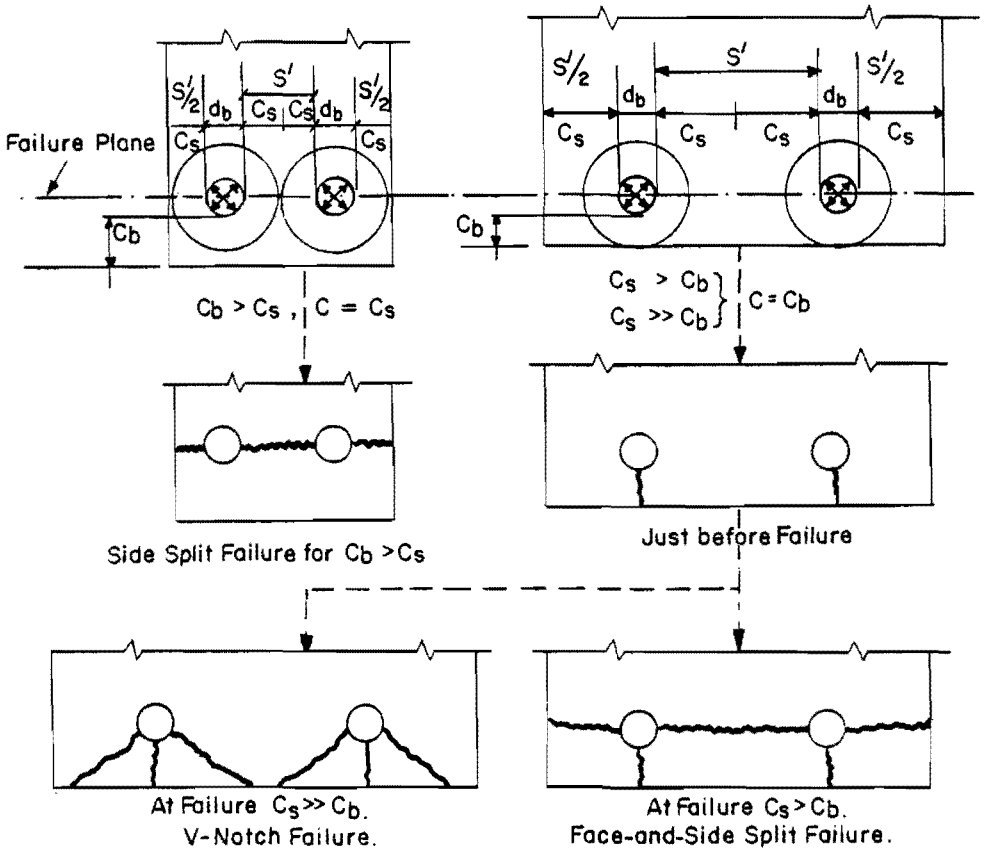

Fig. 2.4 Failure patterns of deformed bars

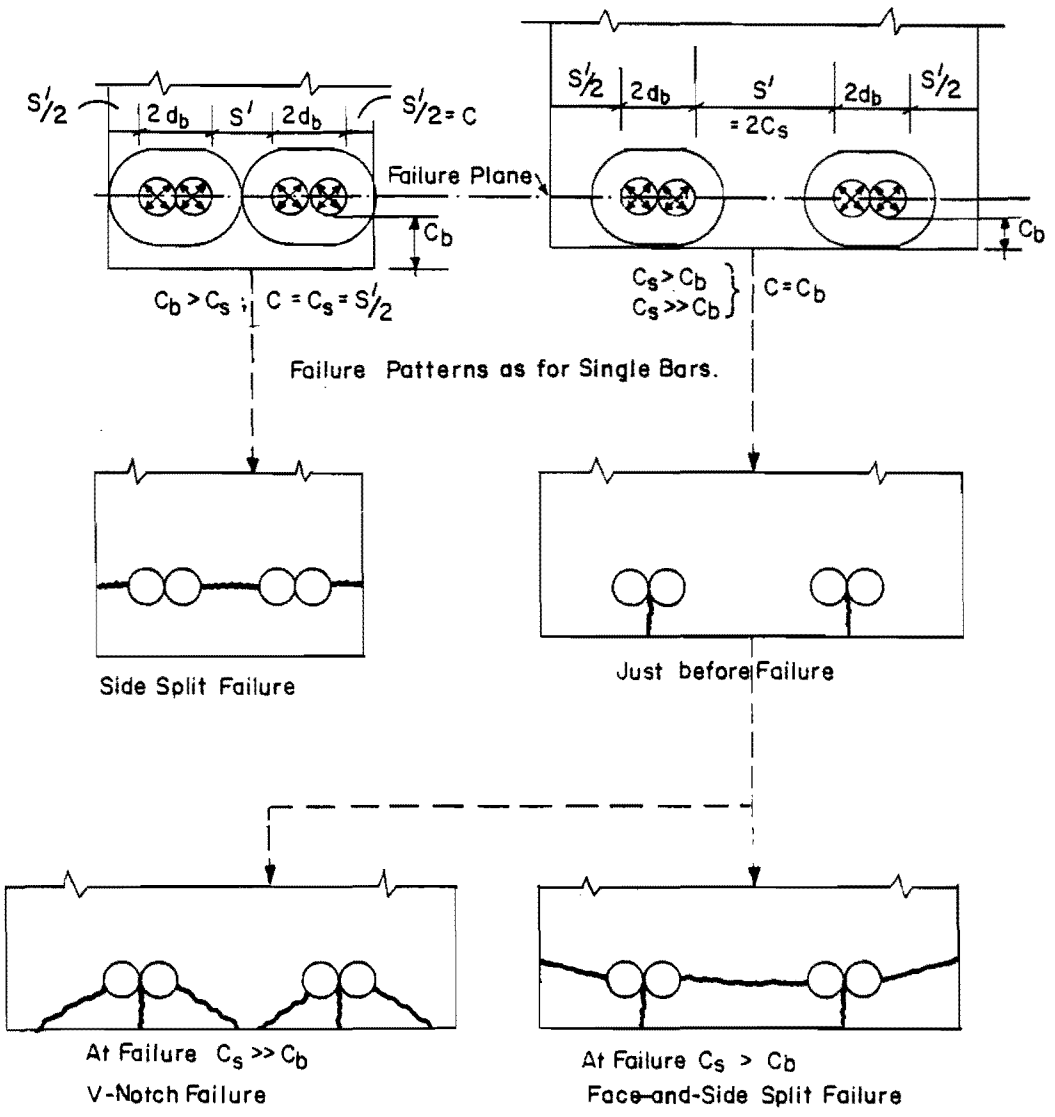

Fig. 2.5 Failure patterns in lapped splices

nondimensional parameters, $u/\sqrt{f_c'}$, C/d_b, and d_b/ℓ_s was developed:

$$\frac{u_c}{\sqrt{f_c'}} = 1.2 + 3\frac{C}{d_b} + 50\frac{d_b}{\ell_s} \tag{2.6}$$

The increase of strength provided by the transverse reinforcement was found to correspond with the following expression:

$$K_{tr} = \frac{u_{tr}}{\sqrt{f_c'}} = \frac{A_{tr} f_{yt}}{500\ s d_b} \tag{2.7}$$

The bond strength was obtained by combining the two expressions:

$$u_{cal} = u_c + u_{tr} \tag{2.8}$$

or

$$u_{cal} = \left[1.2 + 3\frac{C}{d_b} + 50\frac{d_b}{\ell_s} + \frac{A_{tr} f_{yt}}{500\ s d_b}\right] \sqrt{f_c'} \tag{2.9}$$

subjected to the following limitations:

(a) $\frac{C}{d_b} \leq 2.5$

(b) $\frac{A_{tr} f_{yt}}{500\ s d_b} \leq 3.0$

} For large cover or transverse reinforcement the mode of failure changes from splitting to pullout and Eq. (2.9) was based on splitting failures.

(c) For top reinforcement, Eq. (2.6) should be divided by a casting position factor, α, equal to 1.3

where u_{cal} = calculated unit bond stress, psi

u_c = portion of bond strength contributed by the concrete cover, psi

u_{tr} = portion of bond strength contributed by the transverse reinforcement, psi

C = minimum cover, in.

C_b = clear bottom cover to main reinforcement, in.

C_s = half clear spacing between bars or splices, or half available concrete width per bar or splice resisting splitting in failure plane, in.

d_b = bar diameter, main reinforcement, in.

A_{tr} = area of transverse reinforcement crossing the plane of splitting through the anchored bars, $in.^2$

f_{yt} = yield strength of transverse reinforcement, psi

s = spacing of the transverse reinforcement, in.

f'_c = concrete compressive strength, psi

For the transverse reinforcement to be fully effective in improving the splice strength, the transverse reinforcement must be adjacent to and on the outside of the splice in tension and must cross the potential plane of splitting causing failure; A_{tr} must be normal to the splitting crack. Figure 2.6 shows the effectiveness of the transverse reinforcement. In case (a) A_{tr} is only effective for the two edge splices. The value of A_{tr} to be used in Eqs. (2.7) and (2.9) can be calculated as an average effective transverse area for the splice using the following equation:

$$A_{tr} = \frac{\Sigma A_{tr}}{n_s} \tag{2.10}$$

where n_s is the number of spliced bars in a layer, ΣA_{tr} is the area of transverse reinforcement crossing the plane of splitting (see Fig. 2.6).

The length of the bar required to develop f_s can be calculated by equating Eqs. (2.5) and (2.9) and solving for the splice length ℓ_s, the following equation results:

$$\ell_s = \frac{d_b\left[\frac{f_s}{4\sqrt{f'_c}} - 50\right]}{1.2 + 3\frac{C}{d_b} + \frac{A_{tr}f_{yt}}{500\, s_{db}}} \tag{2.11}$$

The same equation is used to determine development length ℓ_d of a bar [1].

To compute the stress f_s that the splice can develop for a given lap length, bar diameter, minimum cover, and concrete strength, Eq. (2.11) can be rearranged to obtain the following equation:

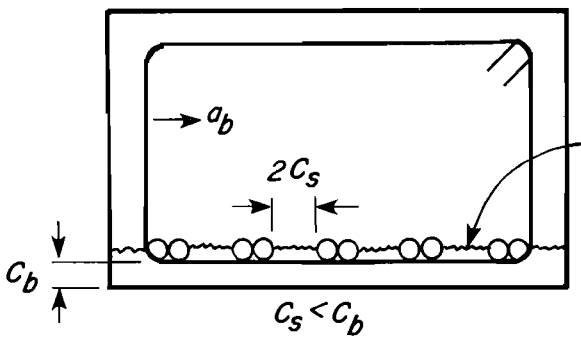

(a) A_{tr} IS EFFECTIVE ONLY FOR TWO OUTER SPLICES

$$A_{tr} = \frac{\Sigma A_{tr}}{n_s} = \frac{2\,a_b}{5}$$

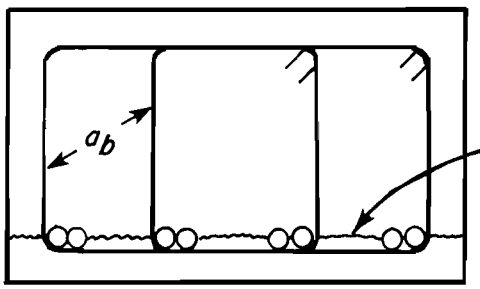

(b) A_{tr} IS EFFECTIVE FOR ALL SPLICES

$$A_{tr} = \frac{4\,a_b}{4} = a_b$$

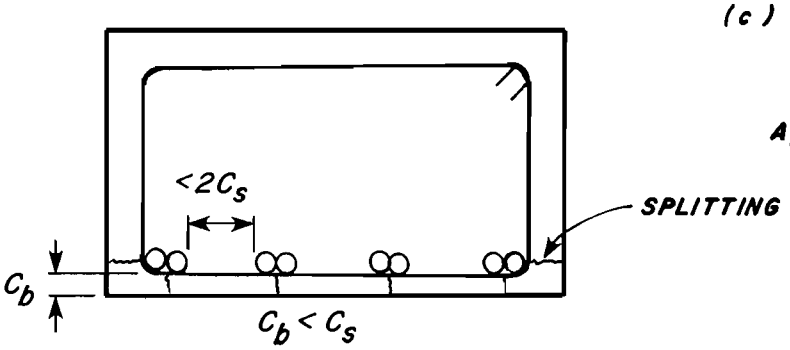

(c) A_{tr} IS EFFECTIVE FOR ALL SPLICES

$$A_{tr} = \frac{4\,a_b}{4} = a_b$$

Fig. 2.6 Definition of transverse reinforcement, A_{tr}

$$f_s = \frac{4\,\ell_s}{d_b}\left[1.2 + 3\frac{C}{d_b} + 50\frac{d_b}{\ell_s} + \frac{A_{tr}f_{yt}}{500\,sd_b}\right]\sqrt{f_c'} \qquad (2.12)$$

Eq. (2.11) was used to compute the length of the splices in this investigation. No strength reduction factor was used in computing the splice length. In computations for splice length, the maximum steel stress, f_s, was taken to be two thirds of specified minimum yield stress. The maximum steel stress in this investigation was limited to ensure a bond failure (concrete splitting) and not a failure by yielding in the steel. This ensures data for evaluation of splice development. In actual practice splice length would be selected to ensure yielding of the reinforcement.

2.3 Effect of Moment Gradient

Briceno [9] and Krishnaswamy [11] conducted tests in which the splice was in a region of varying moment. Krishnaswamy suggested that the bond stress for a bar in a constant moment region be modified (increased) for splices subjected to a moment gradient. In a varying moment zone, a reduced splice length can be computed by multiplying the value of ℓ_s for a splice in a constant moment zone by $(1 + k)/2$, where k is the ratio of the lower to higher bar stress at the splice ends [11]. Lap splices can be designed for the average of the stresses at the splice ends. However, using the assumption by Tepfers that failure of a splice coincides with the failure of a "cylinder" of concrete surrounding the bar, Orangun, et al. [1] suggested that a moment gradient should have little or no effect on the bar stresses at failure and concluded that although Eq. (2.9) slightly underestimates the strength of splices subjected to a moment gradient, the difference is not sufficient to revise Eq. (2.9). It should be noted that in the tests studied by Orangun, et al. [1], splices in the region of variable moment were subjected to a fairly low constant shear force. The splices tested in this project are located in regions of high shear.

2.4 Effect of Changes in Concrete Properties

2.4.1 Slump. After the initial concrete placement and before the hardening of the cement-water aggregate mixture, a segregation of the components of the mixture may take place. The heavier cement and aggregates

tend to settle toward the bottom of the mix, while the air bubbles, particles of low specific gravity, and excess water tend to rise toward the top. As the air particles rise they become lodged under horizontal bars. Sedimentation leads to a much more porous and much weaker concrete mix in the upper layers of concrete relative to the lower layers. The increased water content also adds to this weakening effect. The weakened concrete results in a direct reduction of the ability of the concrete to transfer stress to the steel through the lug bearing mechanism. Air and lightweight particles trapped under the bars or lugs form soft, spongy pockets of very weak concrete. The air pockets reduce the area of bearing between the concrete and the lugs with a resulting loss of bond resistance. The soft concrete on the other hand is easily crushed and allows a great deal of slip before bond resistance is developed.

2.4.2 Presence of High Water Reducing Admixtures. Superplasticizers or high-range water reducing admixtures as they are called are relatively new developments in the field of concrete technology. Superplasticized concrete is conventional concrete containing a chemical admixture of the superplasticizing type. The addition of the admixture imparts unique properties to the concrete. If the superplasticizer is ued to improve workability, the normal slump concrete temporarily becomes "flowing concrete." This is concrete having a slump equal to 8 in. or more for a relatively short time. Bleeding, abnormal retardation, and excess air entrainment should be reduced. Similarly, because of the greatly improved workability, reductions in the water content of superplasticized concrete can be made while maintaining conventional workability levels, namely (2-3 in.) slump. Concrete in this state is sometimes referred to as "water reduced" or "high strength" concrete. Concrete designed to have an initial slump of 3 in. can have slump temporarily increased to something in excess of 8 in. by the addition of a superplasticizer. Due to problems of transporting high-slump concrete, it is very likely that the admixture will be added to the concrete in the mixer truck just before it is used.

No literature is available on the effect of superplasticizers on the behavior of lapped splices. To gain some insight, two exploratory tests with superplasticizer added just before casting were included in this study.

2.5 Current ACI and AASHTO Code Provisions

The current ACI 318-77 Building Code [6] and AASHTO 1979 Interim Bridge Specifications [8] determine splice length by applying factors to the basic development length. The factors depend on (1) the percentage of steel spliced within the lap length, and (2) the ratio of area of reinforcement provided to the area of reinforcement required by analysis. The tension lap splices in this study are classified as Class C splices in ACI 318-77, Section 12.16.2 [6] and in AASHTO 1979 Specifications, Section 1.5.22 [8]. For #11 and #9 bars the required Class C splice length is:

$$\ell_s = 1.7 \cdot \ell_d \cdot \alpha \tag{2.13}$$

or

$$\ell_s = \frac{1.7\ (0.04)\ A_b\ f_y\ \alpha}{\sqrt{f_c'}} \tag{2.14}$$

For top reinforcement, Eq. (2.14) is multiplied by a casting position factor, α, equal to 1.4. By rearranging Eq. (2.14) and solving for steel stress, the following equation is obtained:

$$f_s = \frac{\ell_s \sqrt{f_c'}}{1.7\ (0.04)\ A_b\ \alpha} \tag{2.15}$$

Equation (2.15) was used to compute the stresses from ACI and Code provisions for comparison with the computed stresses obtained in the tests.

CHAPTER 3

EXPERIMENTAL PROGRAM

3.1 Test Specimens

The test program consisted of twelve beams. Each beam was constructed with both bottom and top cast splice test zones. Each test zone will be referred to as a specimen. The basic test specimen is shown in Fig. 3.1 and Table 3.1 summarizes details of the specimens. The concrete strengths ranged from 3700 psi to 5700 psi. The main reinforcing steel was #11 deformed bars in ten beams and #9 deformed bars in the other two beams. The clear cover to the longitudinal reinforcement was 2 in. The minimum side cover to the reinforcement was also 2 in. The clear spacing between the splices was 4 in. for #11 bars and 3 in. for #9 bars. Equation (2.11) was used to determine the required splice length to develop 2/3 f_y or 40 ksi with the critical cover parameter C (the smaller of C_b or C_s), equal to 2 in. for #11 bars and 1.5 in. for #9 bars. The computed splice length was 22 in. for #11 bars and 16 in. for #9 bars.

3.2 Variables

The primary variables were: (1) the level of shear on the splice, (2) the amount and configuration of transverse reinforcement, (3) casting position of the splice (height of bars above bottom of form), (4) the concrete strength, (5) concrete consistency, (6) bar size, and (7) the splice location along the shear span.

3.2.1 Level of Shear. Three different shear spans, 40 in., 53 in., and 80 in., were used. With an effective depth of 13.3 in., the a/d ratios were 3.0, 4.0, and 6.0, respectively. The splice was designed to limit the capacity of the section. The level of shear was limited by the resisting moment developed at splice failure divided by the shear span. The levels of shear were based on the assumption that the splice would develop stresses not greater than 40 ksi.

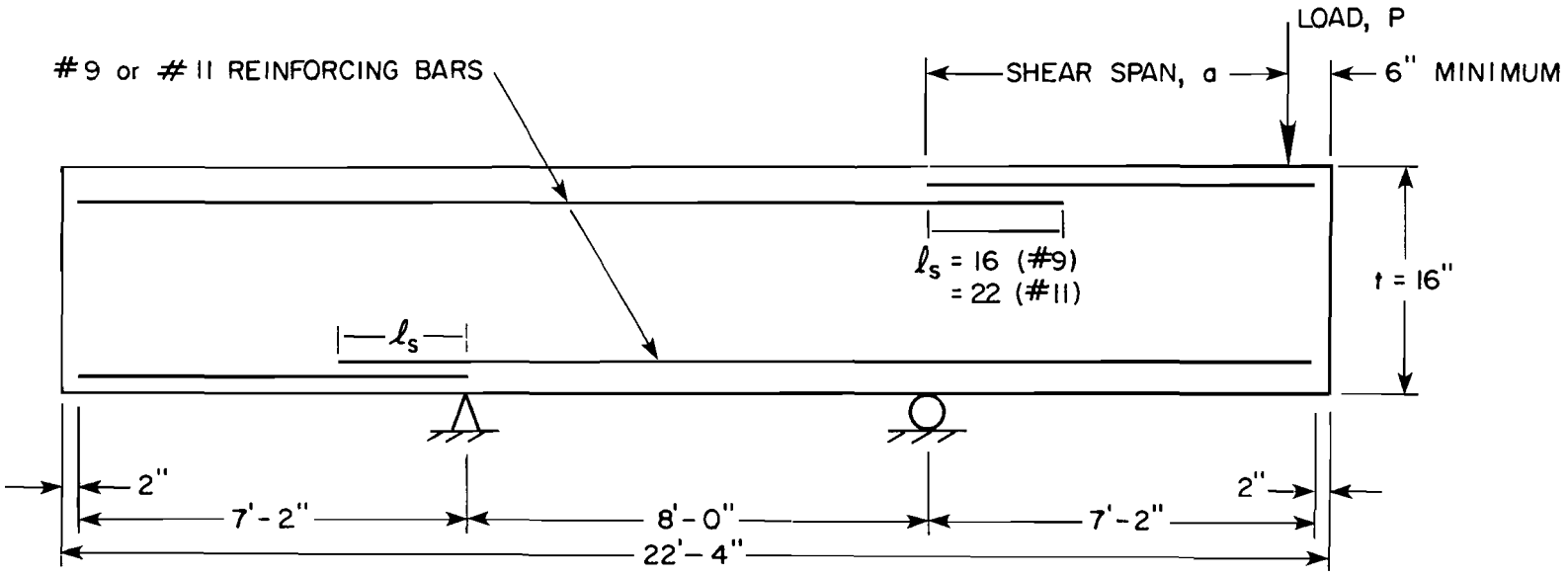

Fig. 3.1 Side view of test specimen (load shown for top cast splice test)

TABLE 3.1 DETAILS OF TEST SPECIMENS

Test No.	Bar Size	Shear Span a (inches)	Concrete		Slump (inches)	f_y (ksi) (Long. Reinf.)	f_{yt} (ksi) (Trans. Reinf.)	Stirrup Size	Stirrup Spacing s (inches)	Number of legs	Casting Position
			Age at Testing (days)	f_c' (psi)							
1	#11	40	66	3700	4.5	60.1	60.3	#3	5	2	top
2	#11	40	75	3750	4.5	60.1	60.3	#3	5	2	bottom
3	#11	53	91	3775	4.5	60.1	60.3	#3	5	2	top
4	#11	53	94	3775	4.5	60.1	60.3	#3	5	2	bottom
5	#11	53	60	4125	7.0	60.1	74.5	6mm	4.5	2	bottom
6	#11	53	63	4150	7.0	60.1	74.5	6mm	4.5	2	top
7	#11	80	44	3825	5.5	60.1	----	---	--	-	top
8	#11	80	45	3825	5.5	60.1	----	---	--	-	bottom
9	#11	80	76	4200	7.0	60.1	74.5	6mm	4.5	2	bottom
10	#11	80	83	4200	7.0	60.1	74.5	6mm	4.5	2	top
11	#11	40	64	3850	5.5	60.1	74.5	6mm	5	4	top
12	#11	40	66	3850	5.5	60.1	74.5	6mm	5	4	bottom
13	#11	53	47	4025	3.5	60.1	70.0	6mm	4.5	2	top
14	#11	53	51	4025	3.5	60.1	70.0	6mm	4.5	2	bottom
15	#11	53	58	4125	3.5	60.1	70.0	6mm	4.5	2	bottom
16	#11	53	64	4125	3.5	60.1	70.0	6mm	4.5	2	top
17	#11	40	55	5425	10.5	60.1	70.0	6mm	4.5	2	top
18	#11	40	57	5425	10.5	60.1	70.0	6mm	4.5	2	bottom
19	#11	40	59	5050	6.5	60.1	70.0	6mm	4.5	2	bottom
20	#11	40	62	5050	6.5	60.1	70.0	6mm	4.5	2	top
21	#9	53	15	5650	7.0	62.8	----	---	--	-	top
22	#9	53	17	5650	7.0	62.8	----	---	--	-	bottom
23	#9	53	21	5700	7.0	62.8	70.0	6mm	4.5	2	bottom
24	#9	53	22	5700	7.0	62.8	70.0	6mm	4.5	2	top

3.2.2 The Transverse Reinforcement. The transverse reinforcement was varied as follows: (a) no transverse reinforcement, (b) the area of steel providing the ACI 318-77 [6] and AASHTO Code [8] minimum v_s (shear strength contributed by transverse reinforcement) of 50 psi, and (c) the area of steel providing twice the Code minimum. The ACI Code minimum area of transverse reinforcement can be provided by two #2 legs @ 4-1/2 in. and twice the minimum corresponds to two #3 legs @ 5 in. The transverse reinforcement provided is greater than that required for the shear force on the section when the splice fails. It is important to note that bond failures and not shear failures were of interest.

The same area of transverse reinforcement could be provided using different configurations. By using a smaller bar size, a greater number of transverse legs is needed to provide the same area. With more legs, more anchored bars may be contained by 90^{o} bends. To study the presumed beneficial aspects of intermediate tie legs, the performance of specimens having two #3 legs @ 5 in. can be compared with specimens having four #2 legs @ 5 in.

3.2.3 Casting Position. The current ACI [6] and AASHTO [8] codes specify that the splice length must be increased by 40 percent for top cast bars with greater than 12 in. of concrete cast below the bar. The top cast splices in this study have 12.6 in. of concrete cast below the bars. In another phase [4] of this overall research project, the effect of casting position on the strength of anchored bars and lapped splices was studied. The results indicated that code recommendations were very conservative for horizontally cast bars. The applicability of those results will be examined for the splice tests reported herein.

3.2.4 Concrete Strength. The correlation between concrete strength and bond strength is not well defined but it is generally accepted that bond strength increases slowly with increase in concrete strength. Since splitting is a tension failure, bond strength should be a function of concrete tensile strength rather than compressive strength (ACI Committee 408). Various investigators have suggested expressions for the bond

strength in terms of $(f_c')^n$ with values of n varying from 0.33 to 0.70, with 0.50 being the most widely used [1,12]. Current provisions of the ACI Building Code [6] and AASHTO specifications [8] base anchorage length requirements on the square root of the concrete compressive strength.

Concrete strength was varied for a number of tests with the same longitudinal and transverse reinforcement, concrete cover, and bar spacing.

3.2.5 Concrete Consistency. In another phase of this overall project [4], it was reported that for normal slump concrete (< 5 in.), the height of the bar above the bottom of the form had little influence on splice and development lengths up to a height of 30 to 40 in. For the beam tests, slump was varied from 3.5 to 10.5 in. In order to achieve a 10.5 in. slump without changing the water/cement ratio and the concrete strength, a HRWR (high range water reducer) "superplasticizer" in powder form was added to the mix before casting.

3.2.6 Bar Size. Research on splices by Tepfers [10] shows that the larger the bar diameter, the lower the splice strength if all other variables remain constant. Earlier work by Chinn, Ferguson, and Thompson [12] showed that when the lap length, beam width, and cover were fixed at a given number of bar diameters, the bond stress developed by a #3 bar was about 19 percent higher than that of a #6 bar and a #11 bar developed bond stress of only 85 percent of a #6 bar. It was suggested [12] that these differences may be due to the fact that the longer the splice, the greater the number of transverse cracks across the length. To investigate this variable, two beams were cast with #9 bars while the remainder were cast with #11 bars.

3.2.7 Splice Location. Cracks form when the principal tensile stresses exceed the tensile strength of the concrete. In a region of large bending moments, these stresses are greatest at the extreme tensile fiber of the member and are responsible for the initiation of flexural cracks perpendicular to the axis of the member. In the presence of shear, significant principal tensile stresses may be generated at approximately 45^o to the axis of the member. The inclined (diagonal tension) cracks

may occur as extensions of flexural cracks. In order to examine the influence of inclined cracking on splice strength, the #11 splices in one beam were located at a distance d from the support where maximum moment is developed, as shown in Fig. 3.2.

3.3 Specimen Geometry

As shown in Fig. 3.1, the beam specimen was a simply supported beam with both ends cantilevered over the supports. This geometry was chosen to permit two separate tests to be run on the same beam by loading the cantilevered ends successively. In this manner, the first test did not disturb or stress the second test zone.

The specimens had the same size bars in the top and bottom faces. The splice length was 22 in. for the #11 bars and 16 in. for the #9 bars. Figure 3.3 shows typical cross sections of the beams. The depth (t), 16 in., was chosen so that at least 12 in. of concrete was cast below the top splices. The width (b), 27-1/4 in., was chosen so that the side cover to the edge bars was 2 in. and the clear space between the splices was 4 in. for #11 bars and 3 in. for #9 bars. The cross section dimensions remained constant for all tests. The total length of each beam was 22 ft., 4 in.

3.4 Materials

3.4.1 Concrete. The concrete mixes used in all the tested beams were based on the Texas Department of Highways and Public Transportation Standard Specification for Class A, non air-entrained concrete with a specific minimum 28 day compressive strength (f_c') of 3000 psi. This standard specifies a slump ranging from 2 to 4 in. However, the slumps were purposely varied and ranged from 3-1/2 to 10-1/2 in.

The specimens were cast with commercially available ready-mix concrete, using Type I Portland cement and Colorado River sand and gravel. The maximum aggregate size used was 5/8 in. Batch proportions and strength gain with time is given in Table 3.2. For one of the specimens an admixture, HRWR (high range water reducer) "superplasticizer," was added to the mix before casting.

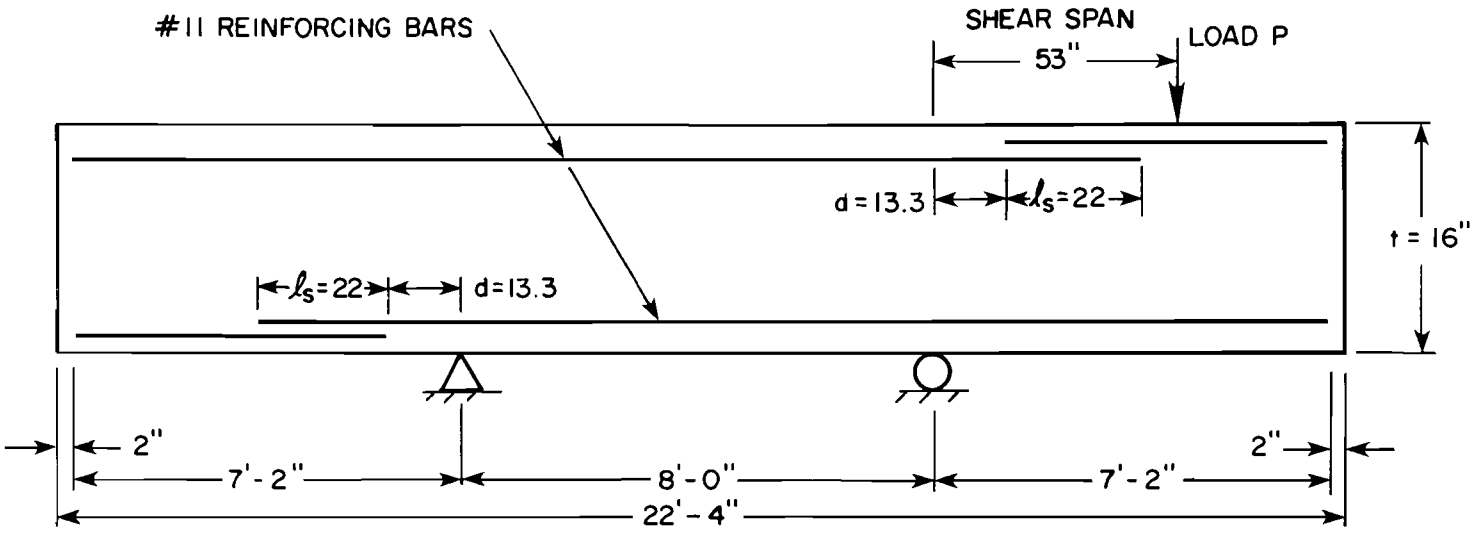

Fig. 3.2 Specimen with splice offset a distance d from support

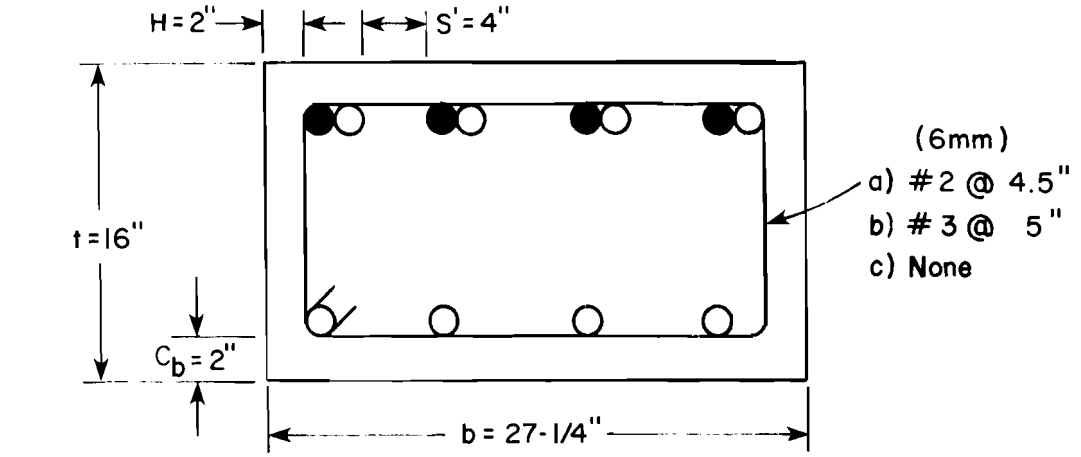

(a) Specimens with #11 bars

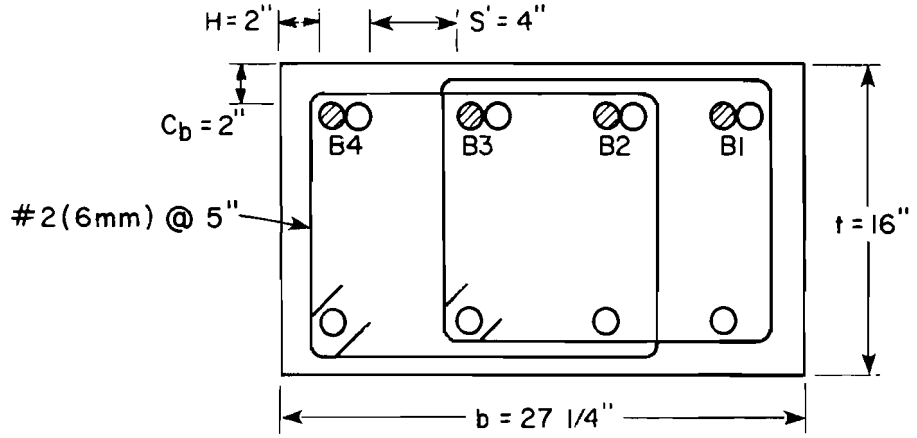

(b) Specimens with #11 bars--four stirrup legs

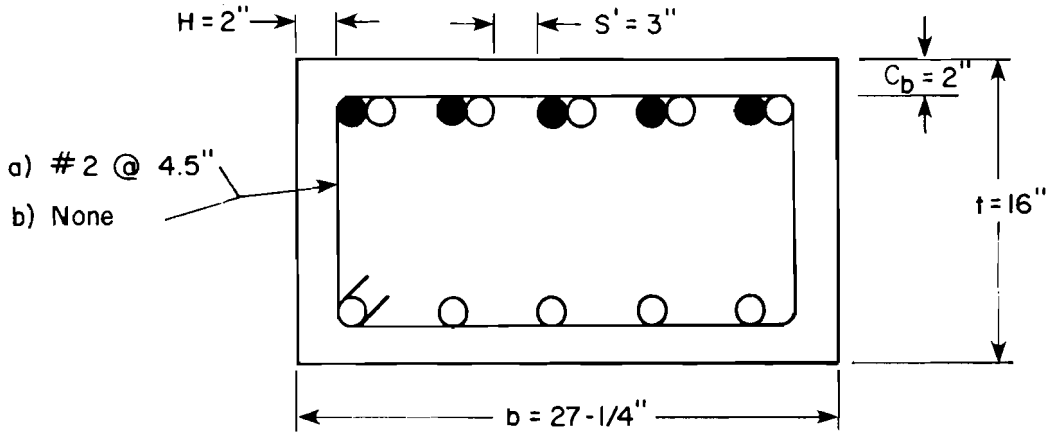

(c) Specimens with #9 bars

Fig. 3.3 Cross section of specimens

TABLE 3.2 CONCRETE PROPERTIES

Tests	Batch Proportions, lb/yd^3				Water Cement Ratio	Slump (in.)	f'_c, ksi			
	Coarse Agg. (5/8")	Fine Agg.	Water	Cement			7 day	14 day	28 day	60 day
1,2,3,4	1930	1550	230	375	0.62	4.5	---	3.25	3.43	3.70
5,6,9,10	1930	1550	230	375	0.62	7.0	3.03	3.5	3.80	4.12
7,8,11,12	1880	1510	270	365	0.74	5.5	2.75	---	3.80	3.70
13,14,15,16	1960	1570	210	380	0.55	3.5	2.75	3.45	3 75	4.10
17,18	1810	1510	245	520	0.47*	10.5*	3.45	4.30	5.08	5.50
19,20	1810	1510	245	520	0.47	6.5	3.73	4.20	4.70	5.05
21,22,23,24	1840	1530	225	530	0.43	6.5	4.28	5.55	5.70†	---

† 22 days
* 0.7 lb/yd^3 superplasticizer added (1/8 lb/sack cement)

3.4.2 Reinforcing Steel. The longitudinal reinforcement consisted of #11 and #9 deformed bars. The transverse reinforcement was fabricated from 6 mm and #3 deformed bars. The #3, #9, and #11 bars met all ASTM A615-76a specifications. The 6 mm bars manufactured in Sweden were obtained from the Portland Cement Association Laboratory in Skokie, Illinois. Figure 3.4 shows the deformations of some of the bars used in the study and the stress-strain curves for the reinforcement.

3.5 Instrumentation

The behavior of the splices and the transverse reinforcement was monitored by electrical resistance strain gages. All longitudinal bars at the critical section (maximum moment) were instrumented. In addition, three sets of splices were instrumented with gages at the third points of the splice length. Selected splices were also instrumented at several locations. Paper-backed strain gages with lengths of 0.64 and 0.32 in. were used for the longitudinal and transverse reinforcement, respectively.

To mount the gages, two bar deformations were filed off and sanded smooth at the gage locations. The loss of metal was kept to a minimum and did not extend into the main body of the bar. The strain gages were attached using Eastman 910 adhesive. The lead wires were soldered to the gage and attached to the bar using a plastic cable tie which prevented the lead wire from being accidentally detached from the strain gage. The gage and lead connections were waterproofed using a silicone rubber sealant and further protected with a polymer-rubber pad.

3.6 Fabrication

The main reinforcement was cut to the proper lengths. No attempt was made to remove rust and mill scale. All of the strain gages were mounted on the bars before the reinforcing cage was fabricated. The stirrup locations were marked on the bars so that the cage would be correctly and quickly constructed. Tie wires were used to hold each lap splice together. The ends of the splices were carefully aligned and the stirrups

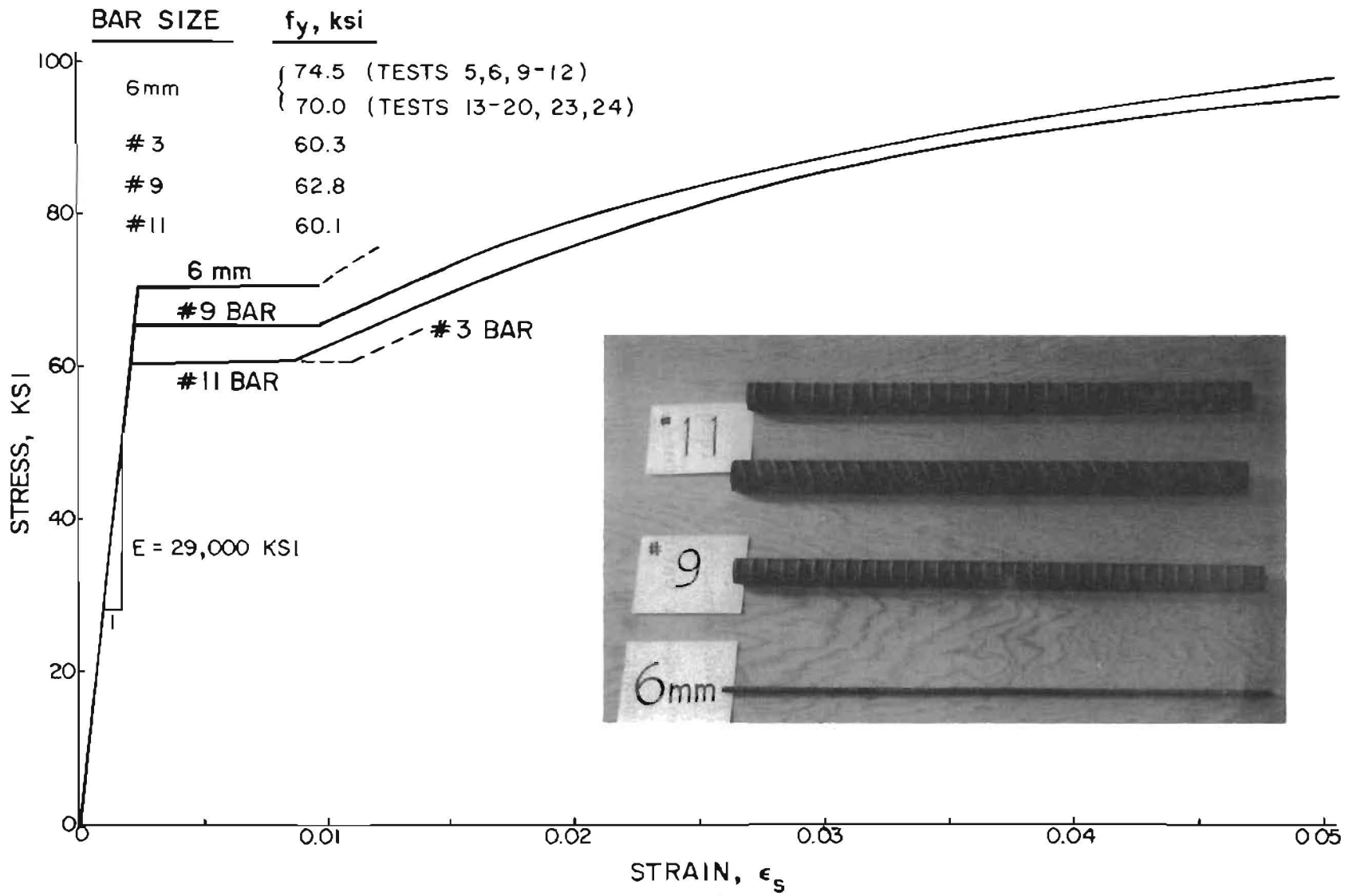

Fig. 3.4 Stress-strain relationship for reinforcing steel

were tied to the longitudinal reinforcement. With the stirrups securely tied, the bottom bars were fed through the stirrups. In beam specimens without transverse reinforcement in the splice zone, the stirrups required to construct the cage were kept a distance d away from the splice. Figure 3.5 shows the reinforcement cages.

Prior to casting the strain gage lead wires were positioned beneath the bars to protect the wires from damage that might occur during the mechanical vibration of the concrete and then bundled together and brought out of the specimen in the central portion of the beam away from the splice region.

3.7 Formwork and Casting Procedure

Two beams were constructed at each casting. The formwork was constructed of 3/4 in. A/B grade plywood braced with construction grade 2 x 4 studs. The center form was common to both beams as shown in Fig. 3.5. The inside faces of the formwork were lacquered to provide a smooth finish. The joints were caulked for watertightness and lightly oiled for easy removal without damage. Chairs or beam bolsters were used to maintain the 2 in. concrete cover to the main reinforcement. No chairs were used in the splice zone. Coil and rod lifting inserts for handling and transporting purposes were positioned near the third points of the beam.

The beams were cast using ready-mix concrete. The slump was measured when the concrete arrived. If necessary, water was added until the desired slump was achieved. The concrete was placed directly from the ready-mix truck and consolidated with mechanical vibrators. The tops of the beams were screeded level and troweled smooth. As the beams were being cast, fourteen standard 6 x 12 in. cylinders were cast. The concrete compressive strength was monitored by taking the average strength attained from testing two cylinders at the time the splice was tested. A time-strength curve was obtained for each casting as indicated in Table 3.2.

After the casting was completed, the beams and the cylinders were covered with a polyethlene sheet and cured for 7 days. The sheet was

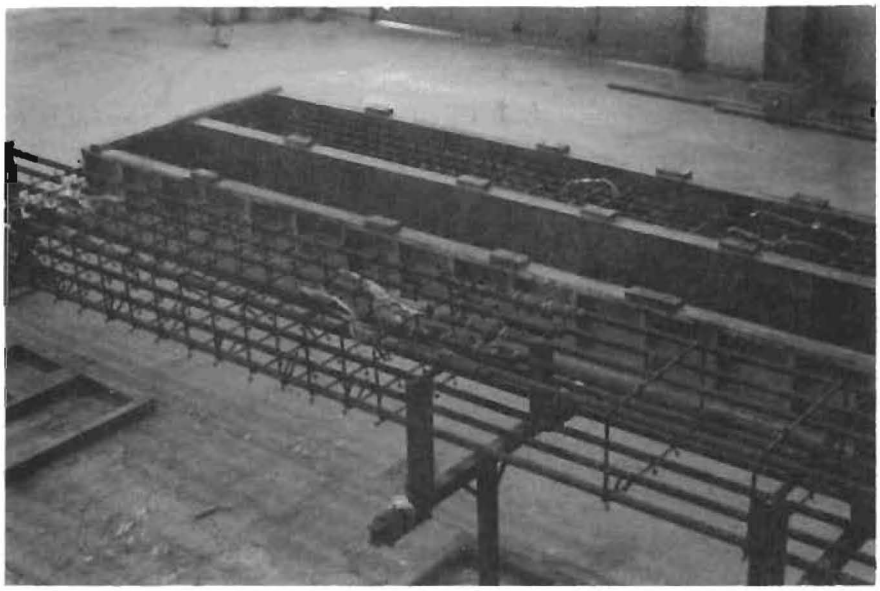

(a) Fabricated reinforcement cage

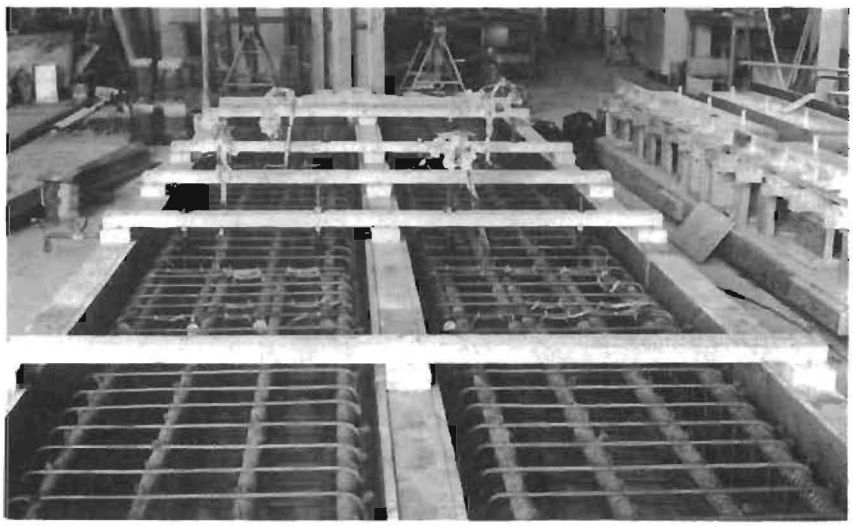

(b) Reinforcing cage in place in form

Fig. 3.5 Reinforcement

removed; the forms were stripped; and the cylinders were removed from the molds after 7 days of curing.

3.8 Test Frame and Loading System

Figure 3.6 shows loading diagrams for the top and bottom splice tests. Because the beams were massive and awkward to handle, the loading arrangement shown in Fig. 3.6 was devised to avoid the need for rotating the beam to test the bottom splice. The test frame is shown in Figs. 3.7 and 3.8. Figure 3.9 shows the test frame and beam in place. The beam was simply supported and loaded on the cantilevered end. The shear level was varied by moving the load point.

The support conditions at the critical section for both the top and bottom splices were the same--simple, pinned end roller connections. The loads were applied to the specimen with two 60 ton double acting hydraulic rams. Equal pressure was supplied to each ram through the use of a manifold connected to a hand pump. The level of load was monitored by a 10,000 psi electronic pressure transducer and a mechanical pressure gage.

In the top splice tests, rams were attached to the reaction beam above the specimen, extending downward to load the specimen. For the bottom splice tests, the rams were positioned on the floor below the beam, extending upward to load the specimen. A very stiff loading bar and plate were used between the rams and the specimen to distribute the load across the beam as uniformly as possible. Grout was used to ensure an even bearing surface between reaction or loading plates and the concrete surface.

3.9 Testing Procedure

The testing procedure was generally the same for all the tests. The test beams were initially loaded in 5 kip increments to approximately one-half of the anticipated failure load. For the remainder of the test, the load increments were reduced to 2 kips. The time interval between load stages varied from 6 to 8 minutes depending on the length of time required to read and record the strain gages. All cracks in the test zone

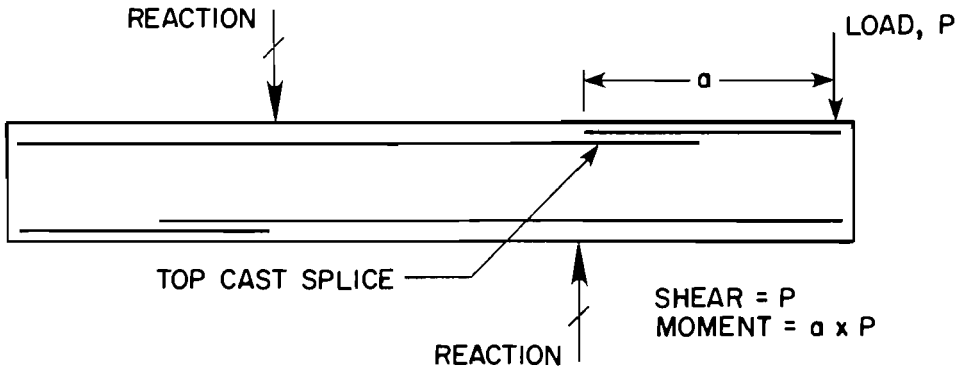

(a) LOADING DIAGRAM FOR TOP SPLICES

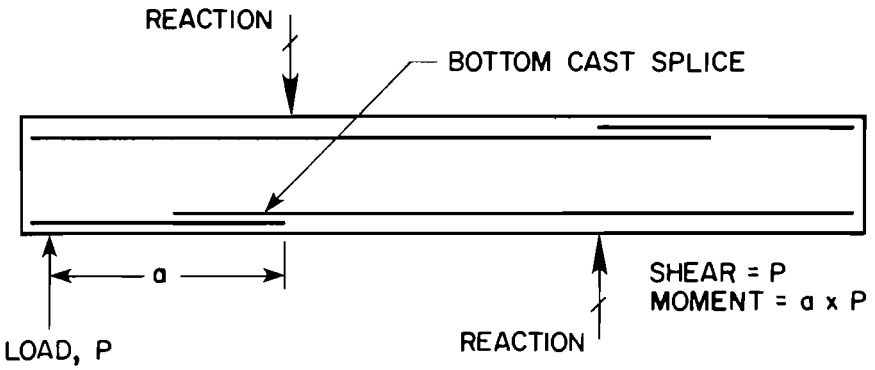

(b) LOADING DIAGRAM FOR BOTTOM SPLICES

Fig. 3.6 Loading diagrams

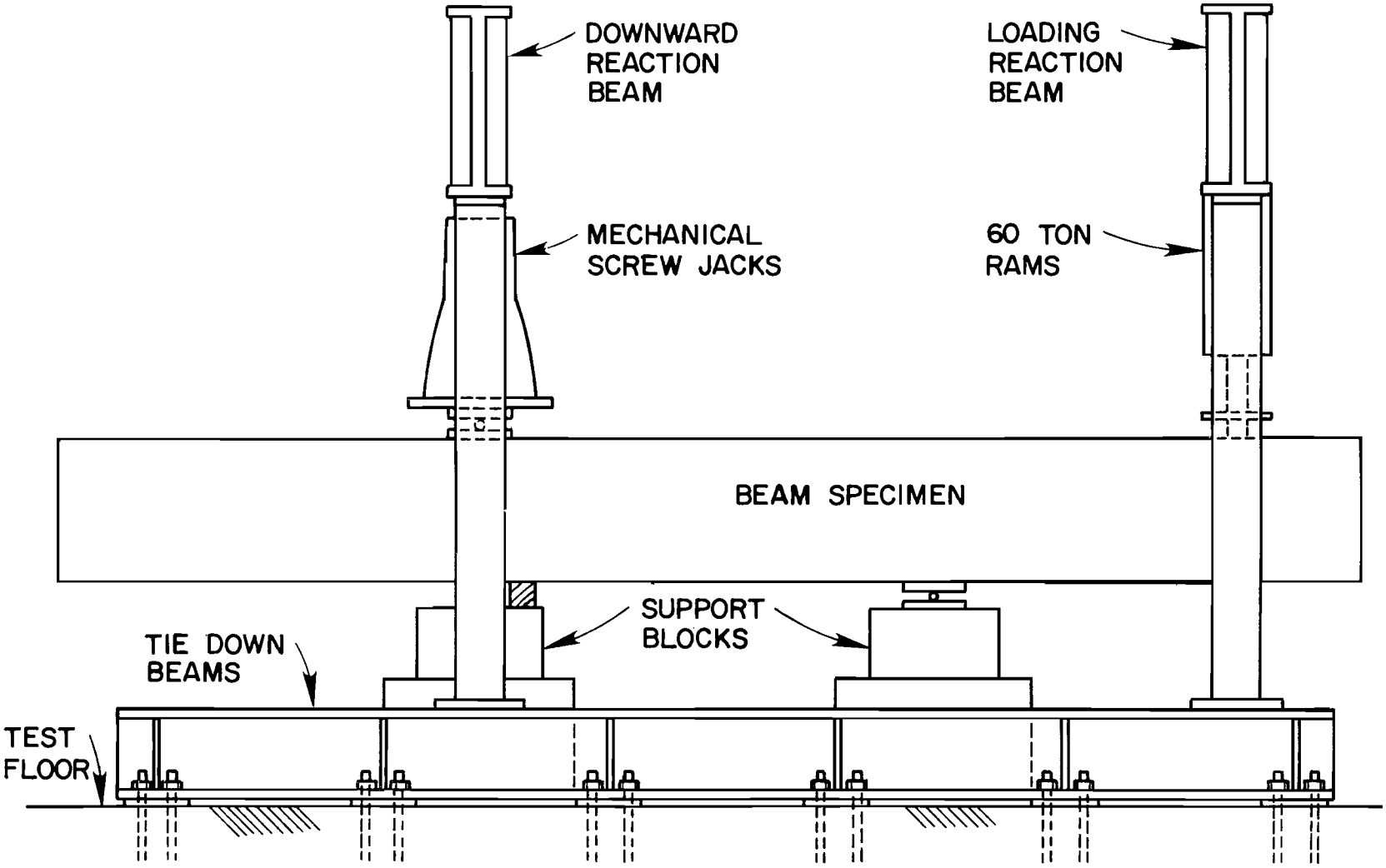

Fig. 3.7 Side view of testing frame (top splice test)

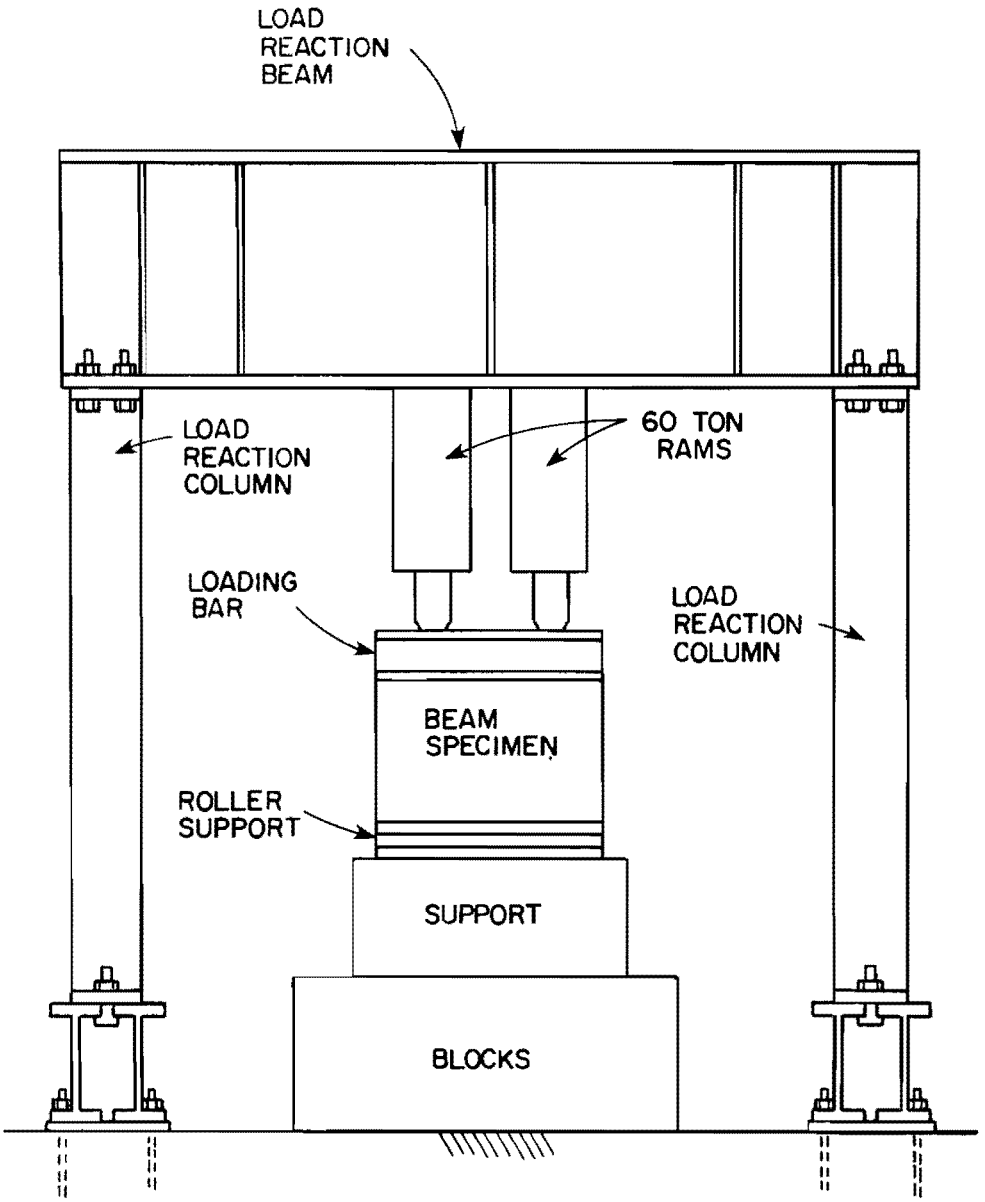

Fig. 3.8 End view of testing frame with rams in place for top cast splice test

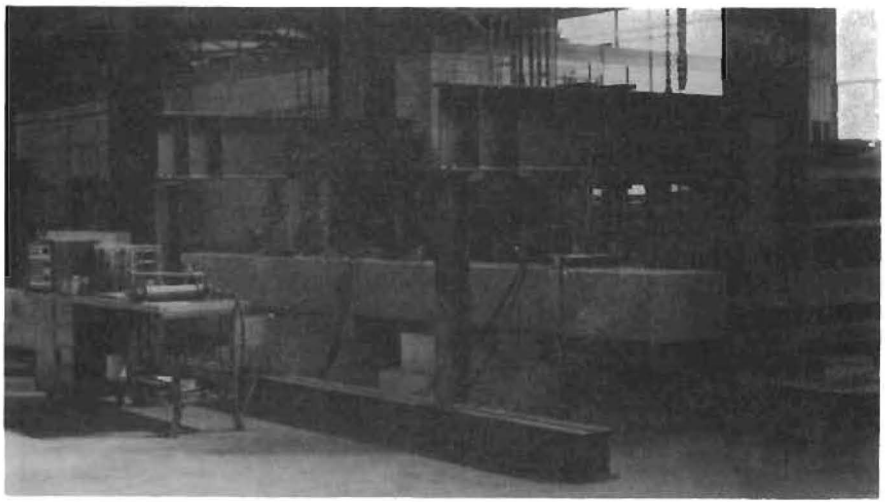

Fig. 3.9 Test frame with a specimen in place

were marked with felt tip pens and labeled to indicate the load stage.

Following failure, a final set of strain gage readings was taken to be used primarily to study the behavior of the transverse reinforcement. The rams were extended to make the failure crack patterns more visible. Upon completion of the test, photographs were taken of both sides and of the tension face of the specimen to record the failure crack patterns.

3.10 Data Reduction

For the interpretation of the test results plots of load vs. strain in the longitudinal and transverse reinforcement were obtained. Adjustments in applied load were made to account for dead load effects.

For comparison of the test results, the load strain data were based on an initial condition of zero stress or strain in the splice. In the position that the beam specimens were tested, the bottom cast splices were initially in compression and the top cast splices were initially in tension.

The amount of dead load moment in each test is shown in Table 3.3.

Since the bottom splices were initially in compression due to the dead load, the axes of the load vs. strain curves were adjusted, as shown in Fig. 3.10a. The load ΔP_{DL}, was dependent on the shear span and the dead load moment (see Table 3.2). As shown in Fig. 3.10a, the strains should be corrected by subtracting $\Delta\epsilon_s$ from the recorded strain data. Because the dead load moments were much less than the cracking moment for the section, the gross transformed section properties were used to compute the dead load strains. The dead load strains were about 1 percent of ϵ_y, a value less than the likely experimental error. Therefore, the adjustments were made only to the loads and the strains were not changed. The top splices were initially in tension due to the dead load and were adjusted as shown in Fig. 3.10b. The values of ΔP_{DL}, summarized in Table 3.3, were added to the recorded loads. No adjustments were made in the strains.

TABLE 3.3 LOAD ADJUSTMENT DUE TO DEAD LOAD MOMENT

Casting Position	Shear Span (in.) (1)	Dead Load Moment (in.-k) (2)	Load Adjustment ΔP_{DL} (kips) (2) ÷ (1)
Bottom	40	-145	-3.6
	53	-145	-2.7
	80	-145	-1.8
Top	40	+150	+3.8
	53	+152	+2.9
	80	+153	+1.9

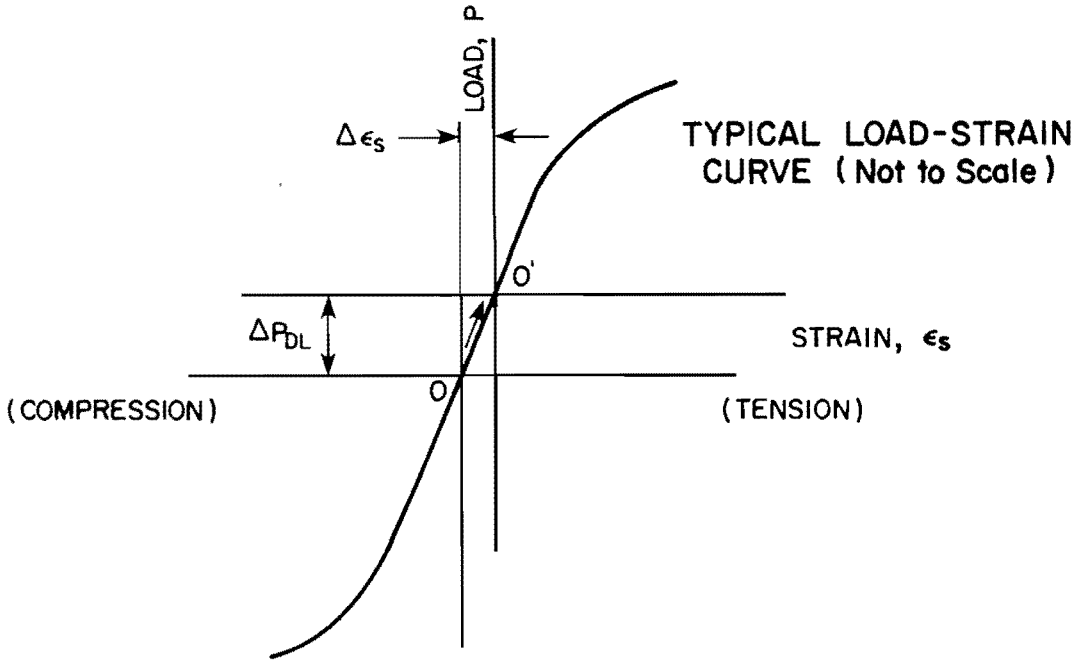

(a) Bottom splices

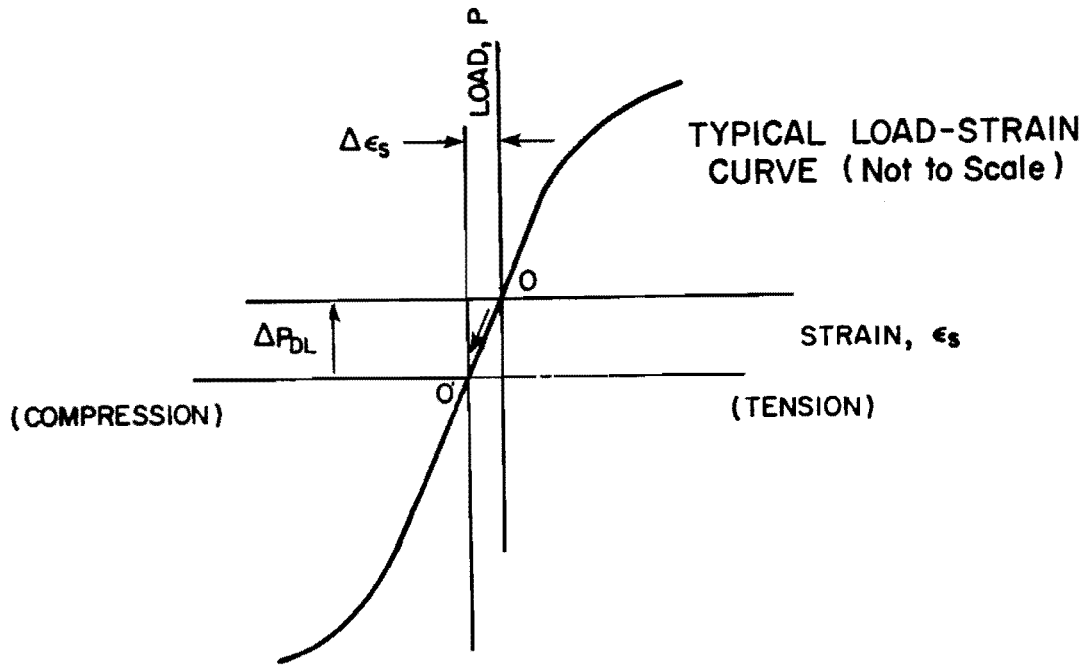

(b) Top splices

Fig. 3.10 Adjustment for dead load strains

CHAPTER 4

SPLICE BEHAVIOR AND TEST RESULTS

4.1 Introduction

The behavior of the lapped splices was evaluated by examining crack patterns at failure and the strains in the reinforcement. Plots of applied load vs. steel strain at selected locations as well as strain distributions across and along the splice were used to study behavior. The behavior and the effectiveness of the transverse reinforcement were studied by using plots of applied load vs. strain in the stirrups. Insight into the behavior of the lapped splices was gained by studying the relation between the progression of cracking and the level of strain in the reinforcement. In general there was close correlation between the cracking patterns and the steel strains. A complete record of all observations is contained in Refs. 15 and 16.

4.2 Crack Patterns

The progression of cracking with increasing load was observed. Cracks were marked at each load stage and numbered. The crack pattern at failure shown in Fig. 4.1 is typical of many specimens. Tensile cracking produced by shear was manifested by diagonal cracks. Splitting cracks on the surface of the specimen produced by anchorage distress were characterized by closely spaced, short low angle diagonal cracks aligned with the axes of the splice. In every test, the first crack to appear on the specimen was a flexural crack at the end of the splice where the moment was greatest. The crack was followed immediately by a similar crack at the other end of the splice. Flexural cracking within the splice zone was fairly evenly spaced. As the load increased, evenly spaced flexural cracks also formed outside of the splice test zone, generally at the stirrup locations. Flexural cracks in the splice zone continued to extend and to bend diagonally toward the support indicating the influence of shear.

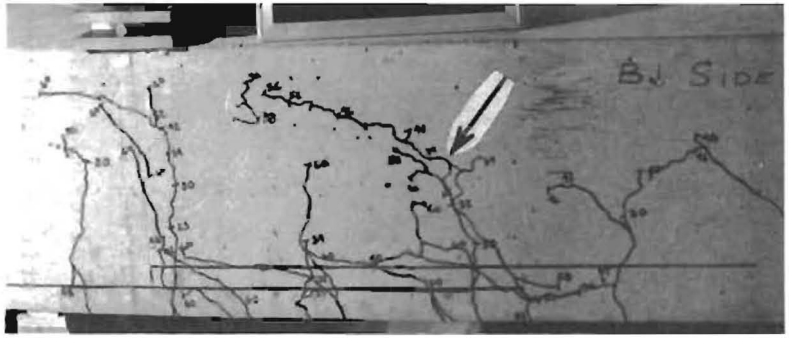

(a) Crack pattern B1 side

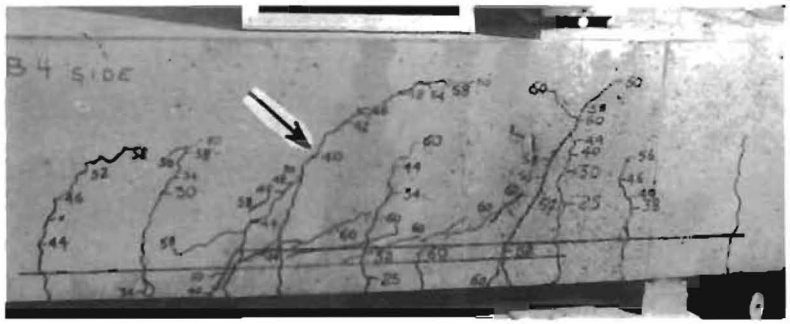

(b) Crack pattern B4 side

(c) Crack pattern on tension face, P_u = 56.9k

Fig. 4.1 Crack patterns, Test #5

Failure of the specimen was imminent when splitting cracks formed in the splice zone. Splitting initiated on the tension face of the specimen at an edge bar. First splitting was usually observed at the end of the splice subjected to the higher stresses. As the load increased, splitting cracks formed on the side of the specimen. When the splitting cracks began to extend rapidly, bond was lost along the splice and the load dropped off substantially. Failures were quite sudden with little warning except for the growth of the splitting cracks.

Two modes of failure were observed, (1) side split mode (Fig. 4.2a), and (2) main face and side face split mode (Fig. 4.2b). These failure modes were described by Thompson, et al. [13] in a previous study on splice failures. In the side split mode, shown in Fig. 4.2a, the vertical clear cover is greater than the edge cover. The cover over the splice exhibits no splitting distress prior to failure. Splitting distress appears as side splitting cracks. Upon failure of the splice, the splitting proceeds horizontally until the cover concrete over the tension reinforcement is lifted with no longitudinal cracking in the cover. In the main face and side face split mode, shown in Fig. 4.2b, initial splitting occurs in the vertical clear cover over the edge splices, presumably both edges. As horizontal splitting cracks develop on the sides, the edge blocks of the concrete tend to break loose, destroying the bond along the outside edge splices. The remaining interior splices then fail by lifting of the clear cover over the reinforcement.

In most of the tests conducted in this study, the failure was generally a main face and side face split mode with a slight variation. The initial splitting visible on the top or bottom surface of the specimen occurred at only one edge splice (see Fig. 4.3). Failure of the remaining bars was produced by lifting of the clear cover over the reinforcement.

After failure, longitudinal and diagonal cracks in the tension face appeared when the rams were extended to make the failure crack patterns more visible. These cracks were due to the redistribution of the internal stresses caused by the failure of the edge splice.

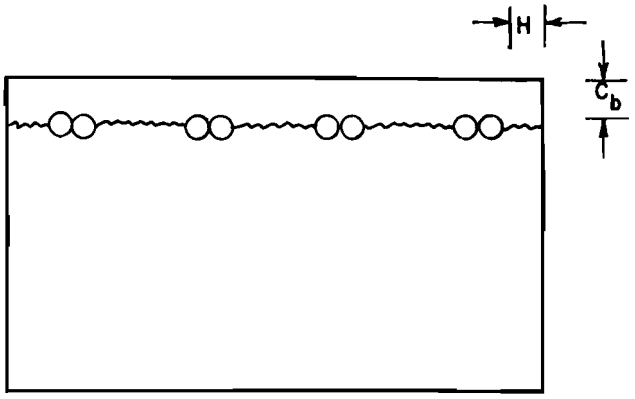

(a) Side split mode ($H < C_b$)

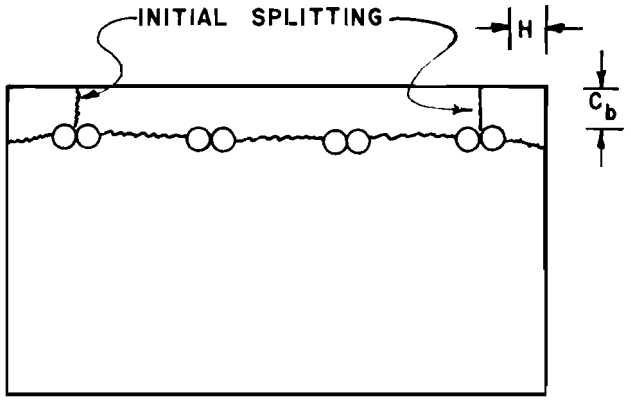

(b) Main face and side face split mode
($C_b \leq H \leq 2C_b$)

Fig. 4.2 Modes of splitting failure

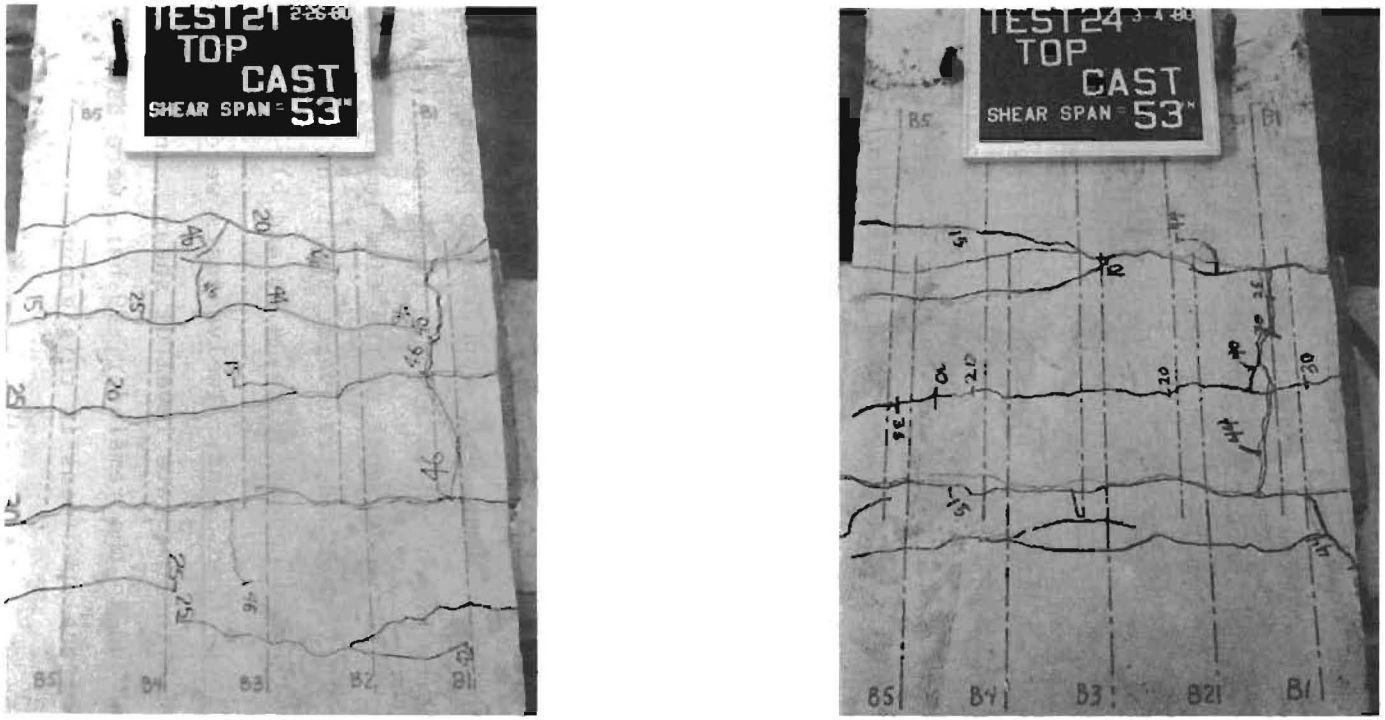

Fig. 4.3 Tension face splitting--one edge only

In order to discuss the cracking behavior of the individual beams, the tests are grouped by shear span because the level of shear influenced the amount of diagonal cracking on the side faces of the specimens.

4.2.1 40 Inch Shear Span. Eight tests were conducted with 40 in. shear spans. These specimens were subjected to the highest shear forces. Figures 4.4 and 4.5 show the cracking patterns on the side of the beams. All crack patterns were similar in that diagonal shear cracks were dominant.

Very few flexural cracks form except near the support. At loads less than 50 percent of ultimate, cracking was limited to the tension face with cracks extending across the face. Very little cracking occurred on the sides until the higher loads were reached, at which point the cracks began to extend at approximately 45° angles reflecting the high level of shear.

Figures 4.5a and b show the crack patterns in the beam in which the superplasticizer (HRWR) was added. The bottom splices (Test 18) could not be taken to failure because loads exceeded the allowable loads for stable operation of the loading frame. It is surmised that the addition of the superplasticizer and the resulting high slump (10-1/2 in.) produced concrete around the bottom splice which had greater strength than around the top splice. The superplasticizer appeared to produce considerable concrete sedimentation which led to a large variation in concrete strength from top to bottom of the specimen. At the time loading was stopped, side splitting had just initiated and transverse splitting across the ends of the splice was starting to appear (Figs. 4.5a and b).

4.2.2 53 Inch Shear Spans. Twelve tests were conducted using a 53 in. shear span, an intermediate level of shear. In eight tests, #11 splices were tested and in the remainder, #9 bars were used. Figures 4.6 and 4.7 show some of the specimens in this group.

Diagonal shear cracks formed at approximately two-thirds of ultimate. Some of the inclined cracks propagated from the flexural cracks and others

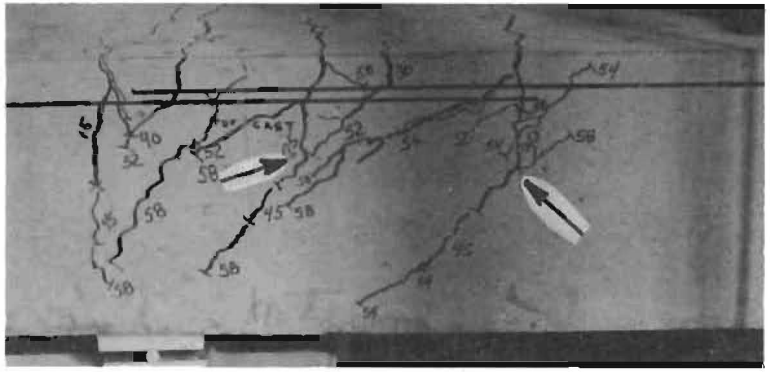

(a) Test 1, top cast, two #3 @ 5 in.

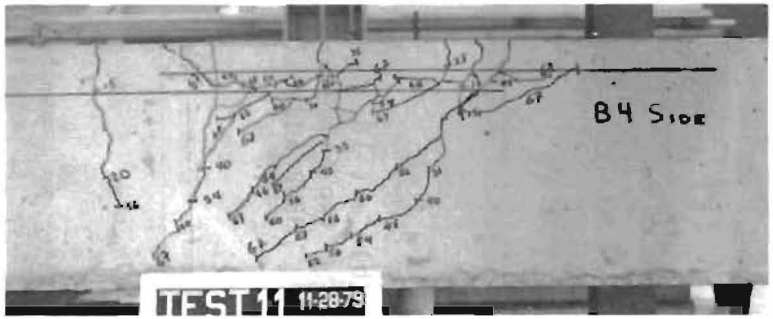

(b) Test 11, top cast, four 6mm @ 5 in.

(c) Test 2, bottom cast, two #3 @ 5 in.

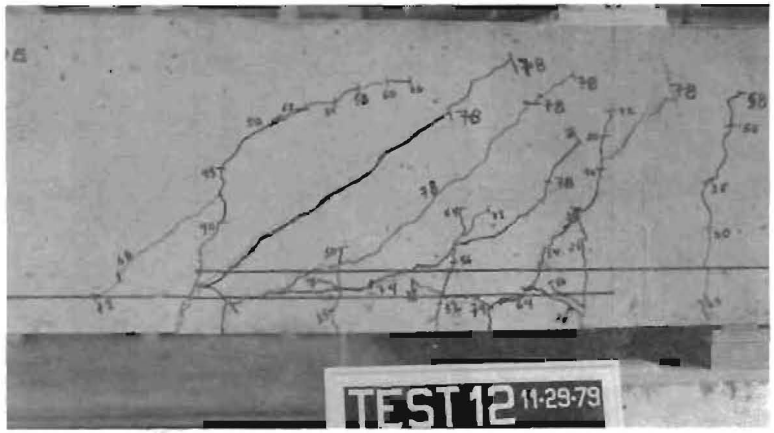

(d) Test 12, bottom cast, four 6mm @ 5 in.

Fig. 4.4 Crack patterns, 40 in. shear span, #11 bars, $f'_c \approx 4$ ksi

(a) Test 17, top cast, two 6mm @ 4.5 in., HRWR added (high slump)

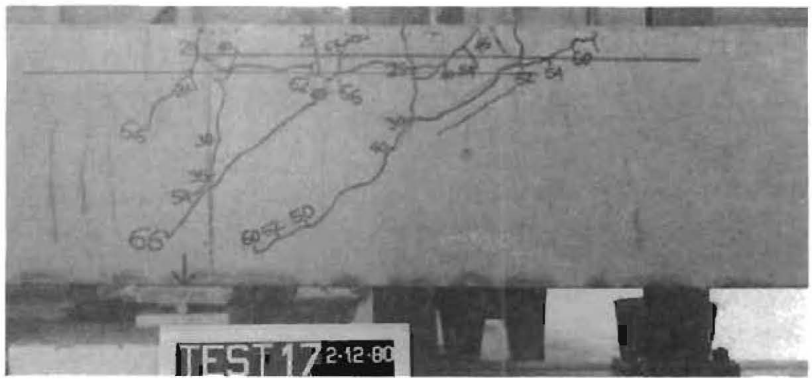

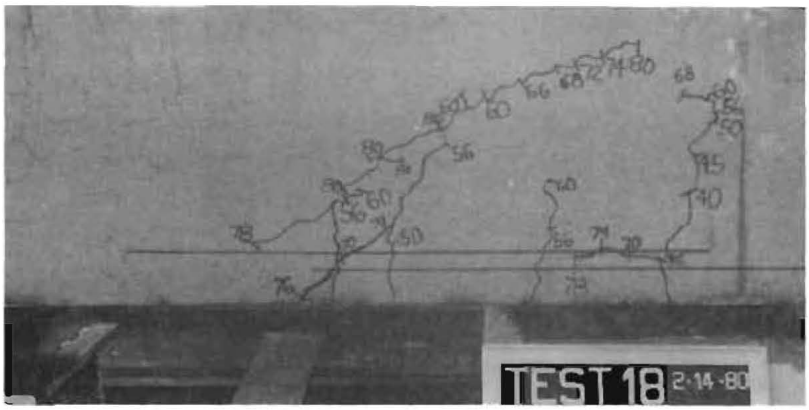

(b) Test 18, bottom cast, two 6mm @ 4.5 in., HRWR added (high slump)

(c) Test 19, bottom cast, two 6mm @ 4.5 in.

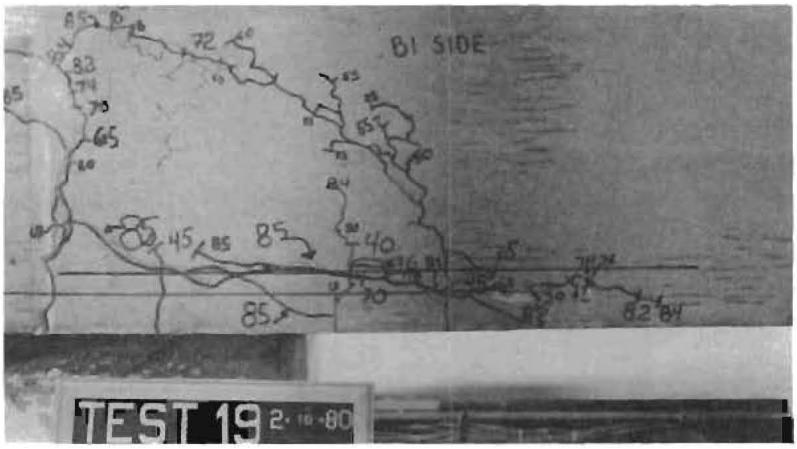

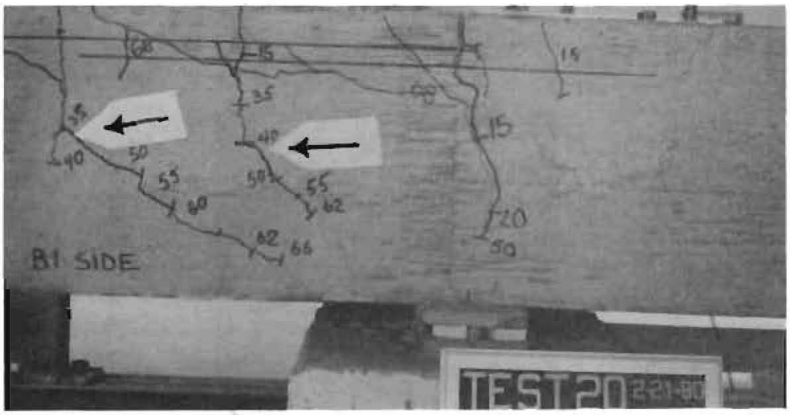

(d) Test 20, top cast, two 6mm @ 4.5 in.

Fig. 4.5 Crack patterns, 40 in. shear span, #11 bars, $f'_c \approx 5$ ksi

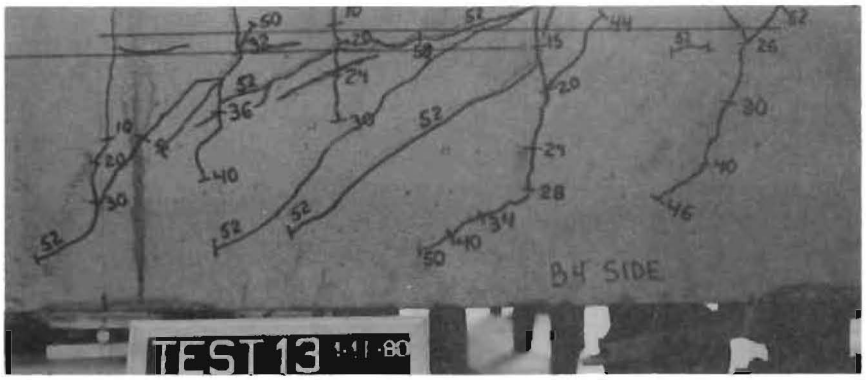

(a) Test 13, top cast, two 6mm @ 4.5 in.

(b) Test 14, bottom cast, two 6mm @ 4.5 in.

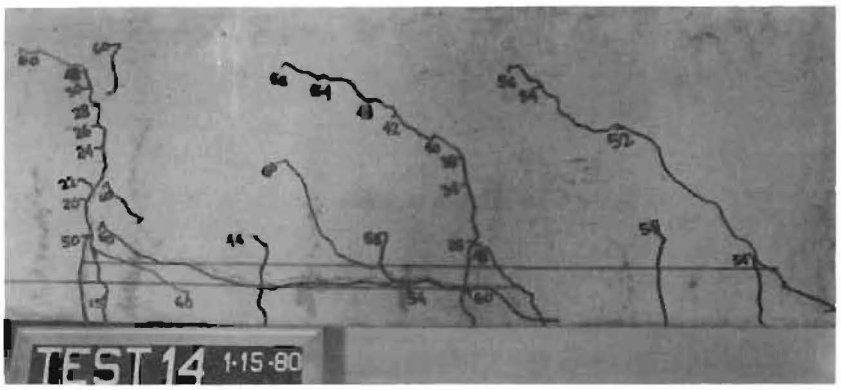

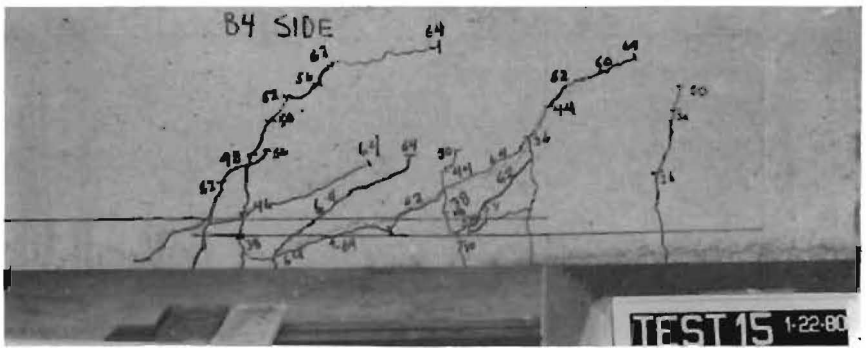

(c) Test 15, bottom cast, two 6mm @ 4.5 in., shifted splice

(d) Test 16, top cast, two 6mm @ 4.5 in., shifted splice

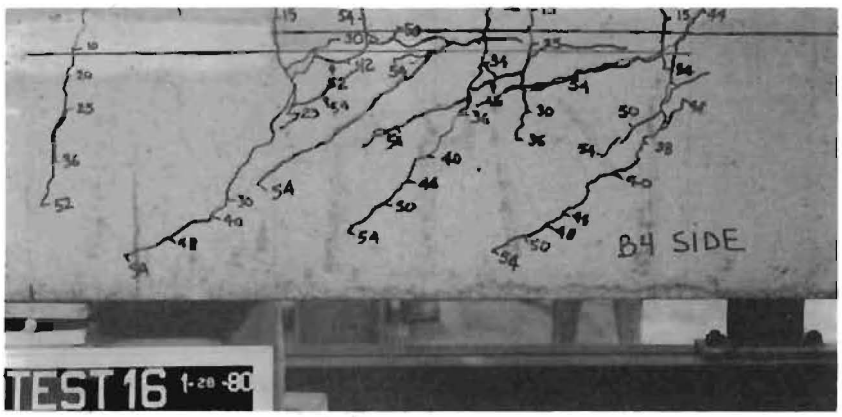

Fig. 4.6 Crack patterns, 53 in. shear span, #11 bars, $f'_c \approx 4$ ksi

(a) Test 21, top cast, no transverse reinforcement

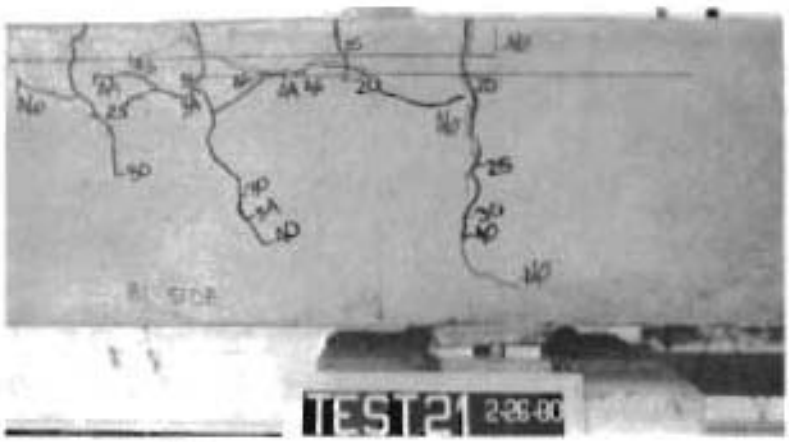

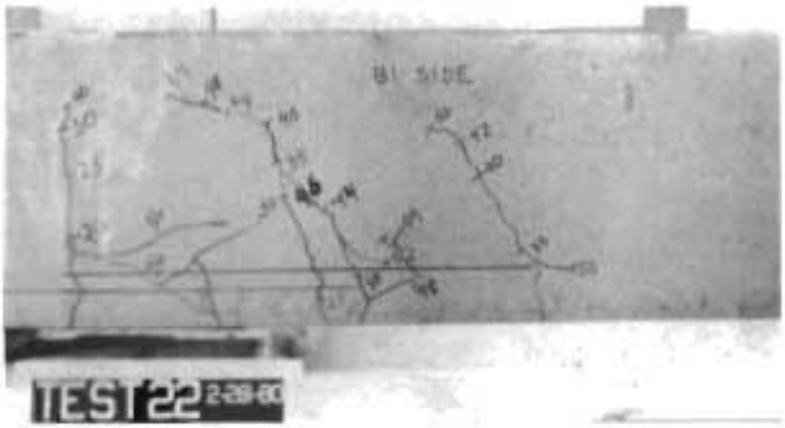

(b) Test 22, bottom cast, no transverse reinforcement

(c) Test 23, bottom cast, two 6mm @ 4.5 in.

(d) Test 24, bottom cast, two 6mm @ 4.5 in.

Fig. 4.7 Crack patterns, 53 in. shear span, #9 bars, $f'_c \approx 6$ ksi

extended from the splitting cracks in the splice region. Splitting on the sides of the specimens was more pronounced than in the specimens tested on 40 in. shear spans.

Four tests were identical except that in Tests 13 and 14 the splice started at the support and in the other two (Tests 15 and 16) the splice was shifted a distance d away from the support. It is interesting to note that the crack patterns for the offset splices were similar to those of the control tests except that the cracks were offset to the splice location. Figure 4.6 shows that flexural cracks formed at the support and (at almost the same loading) appeared at both ends of the splice. As load progressed intermediate flexural cracks appeared at even intervals along the splice. The diagonal crack pattern along the splice was similar regardless of the splice location in the shear span.

In the four test specimens with #9 splices, the transverse reinforcement was varied. Two tests had #2 @ 4.5 in. (Tests 21 and 22) and the other two had no transverse reinforcement (Tests 23 and 24). The crack patterns shown in Fig. 4.7 were similar in that flexural cracking extended approximately half the depth of the beam before diagonal shear cracking developed. There was little difference between the crack patterns for specimens with and without transverse reinforcement. There was a noticeable decrease in both flexural and diagonal shear cracking compared with that observed in the tests with #11 splices.

4.2.3 80 Inch Shear Spans. Four tests, two with bottom cast and two with top cast splices, were tested using 80 in. shear spans. These specimens were subjected to the lowest levels of shear considered in the series. The amount of transverse reinforcement along the splice varied, Tests 7 and 8 had no transverse reinforcement, and Tests 9 and 10 had the minimum amount of transverse reinforcement required by the ACI and AASHTO codes. The crack patterns are shown in Fig. 4.8. Flexural cracking was dominant with inclined cracks forming near failure. Cracking on the side faces remained nearly vertical as the load increased. The inclined shear cracking propagated from the flexural cracks and the splitting cracks

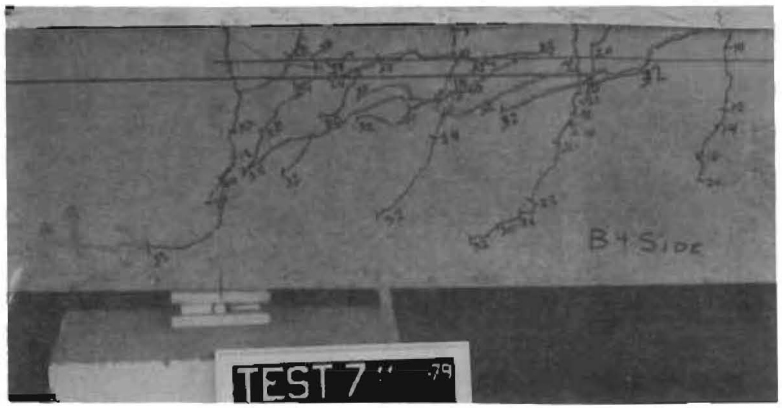

(a) Test 7, top cast, no transverse reinforcement

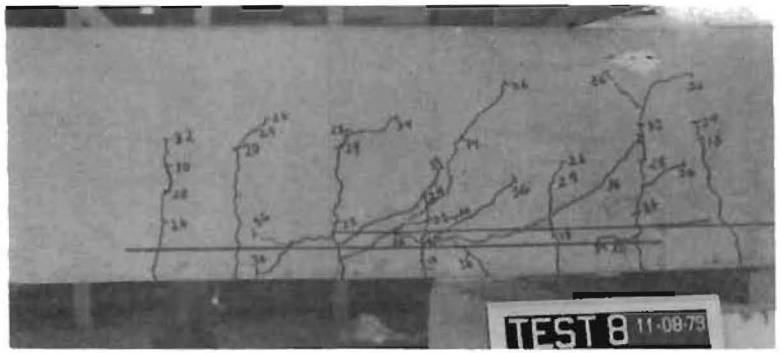

(b) Test 8, bottom cast, no transverse reinforcement

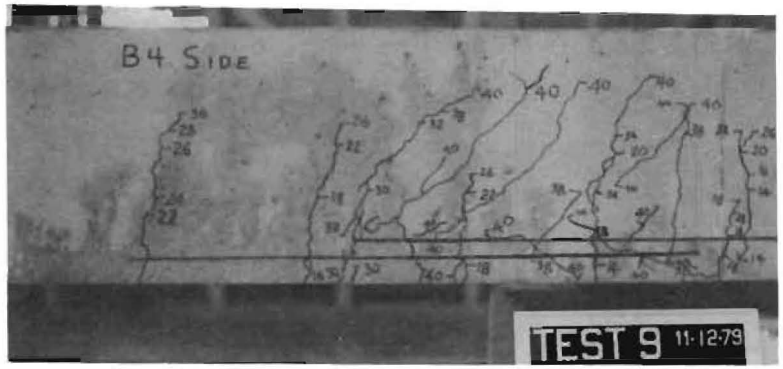

(c) Test 9, bottom cast, two 6mm @ 4.5 in.

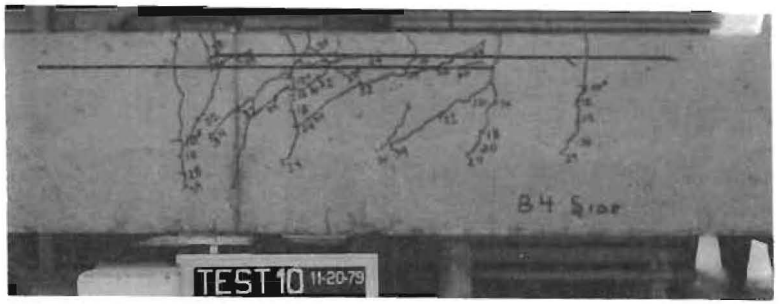

(d) Test 10, bottom cast, two 6mm @ 4.5 in.

Fig. 4.8 Crack patterns, 80 in. shear span, #11 bars, $f'_c \approx 4$ ksi

in the splice zone. At failure the shear cracks became extensions of splitting cracks. Splitting was more pronounced in the specimens without transverse reinforcement than in those with minimum transverse steel.

4.3 Strains in the Longitudinal Reinforcement

To verify the accuracy of the measured strain, the average of the strains measured in the reinforcement (all longitudinal bars) was compared with the average strain calculated from the total applied loads (or moments) on the section. Two methods were used to calculate the average strain in the steel from the applied loads. The first method involved using a cracked transformed section analysis for the beam specimen which resulted in a linear relationship between the applied load (moment) and the average strain in the reinforcement. It was assumed that the stress-strain relationship in the concrete was linear and that the concrete carried no tension. In the second method the average strain in the steel was calculated using a program (PIER 14) which included the effects of cracking in the concrete and a nonlinear stress-strain relationship for the concrete in compression. Figure 4.9 shows the computed strain in the flexural steel in a beam specimen with a 53 in. shear span using both methods. The two lines converge when yield is reached. At low loads, the concrete is carrying a significant portion of the total tensile forces on the cross section and the response is nonlinear. However, as loads and strains increase, the relationship becomes nearly linear.

Table 4.1 summarizes the steel strains at failure for the twelve tests. The table includes the concrete strength, ultimate load, average measured strains in the bar at failure, and the calculated average bar strains at ultimate. The loads and strains shown in Table 4.1 and Fig. 4.9 are adjusted for dead load (see Sec. 3.10).

At low levels of load, the observed strains generally compared well with the calculated strains using the PIER program. The differences were greatest in tests with high levels of shear, i.e. short shear spans.

In order to explain the difference between measured and calculated steel strains, it is useful to look at the level of shear in each test.

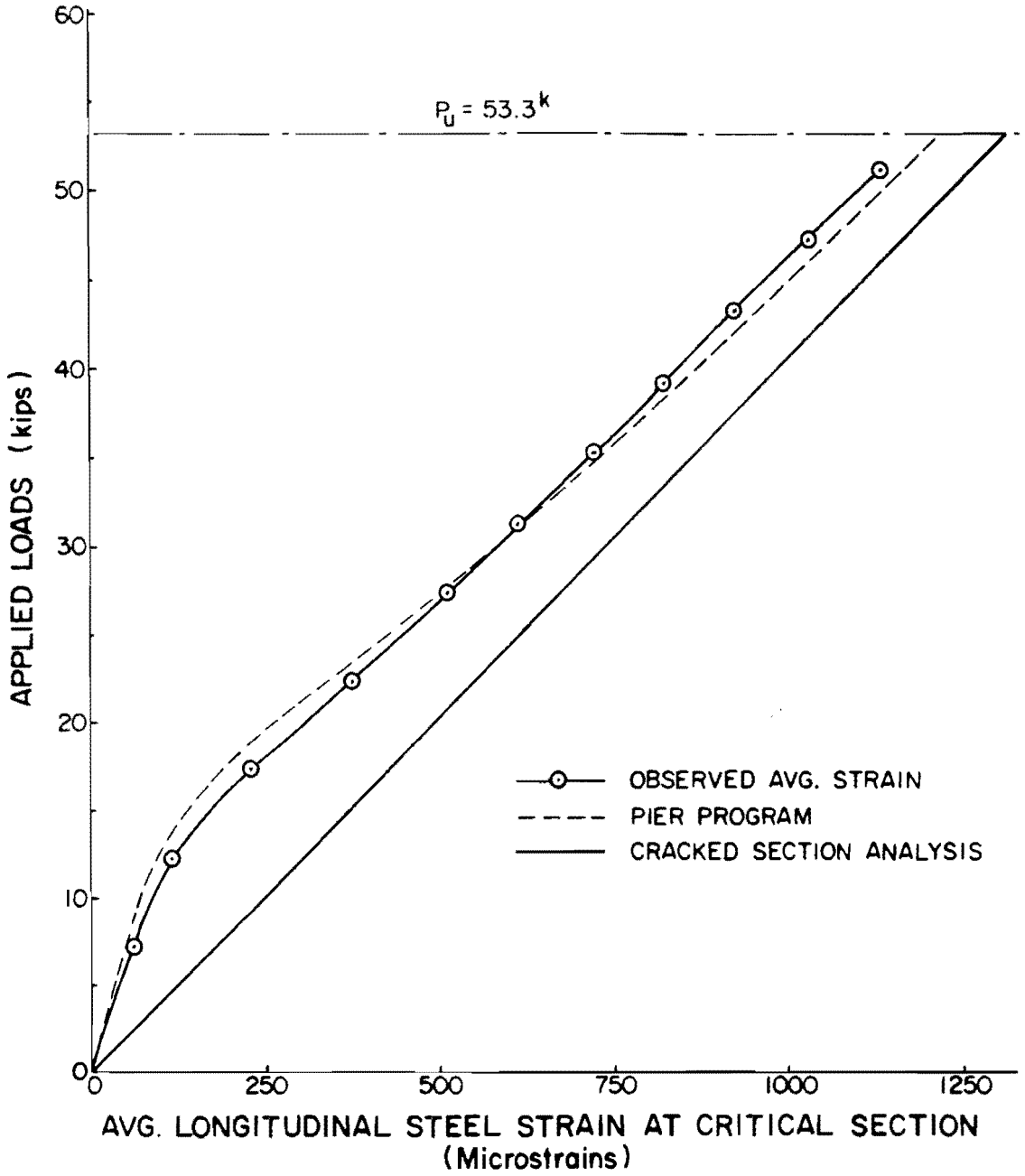

Fig. 4.9 Load vs. strain, Test #4, 53 in. shear span

TABLE 4.1 SUMMARY OF STEEL STRAINS AT FAILURE

Test No.	Test Designation	Concrete Strength f'_c (psi)	Ultimate Load P_u (kips)	Average Measured ϵ_s (Microstrain)	Calculated ϵ_s PIER $f_t \neq 0$ (Microstrain)	Calculated ϵ_s Cracked[3] Section (Microstrain)
1	3-5-40-T	3700	61.8	910	1100	1150
2	3-5-40-B	3750	68.4	1130	1230	1270
3	3-5-53-T	3775	50.9	980	1170	1250
4	3-5-53-B	3775	53.3	1130	1230	1310
5	2-4.5-53-B	4125	56.9	1370	1330	1400
6	2-4.5-53-T	4150	52.9	1110	1230	1300
7	N-N-80-T	3825	33.9	960	1200	1260
8	N-N-80-B	3825	34.0	1220	1200	1260
9	2-4.5-80-B	4200	38.2	1400	1370	1420
10	2-4.5-80-T	4200	35.9	1080	1280	1340
11	2-5-40-T(4)	3850	70.6	1060	1280	1310
12	2-5-40-B(4)	3850	74.5	1210	1360	1390
13	11-53-T	4025	55.0	1460	1280	1470
14	11-53-B	4025	57.3	1380	1330	1530
15[2]	11-53-B-D	4125	61.3	1090	1080	1240
16[2]	11-53-T-D	4125	57.0	1120	1000	1150
17	11-40-T-A	5425	68.0	940	1230	1220
18	11-40-B-A	5425	81.3[1]	1340	1490	1460
19	11-40-B	5050	82.3	1370	1510	1540
20	11-40-T	5050	71.0	1160	1290	1330
21	9-53-T-N	5650	49.0	1300	1370	1480
22	9-53-B-N	5650	53.3	1540	1510	1610
23	9-53-B	5700	64.3	1710	1870	1940
24	9-53-T	5700	47.2	1210	1300	1430

Notes: [1]Load on Test 18 before reaching test frame capacity.

[2]Computed and measured values at a distance d away from critical section.

[3]With tensile capacity of concrete assumed zero.

Since the differences were most pronounced in the tests with high levels of shear, it is possible that shear distortion occurred and that the longitudinal bars were subjected to local bending due to shear distortion as well as tension due to flexure on the section. The strain distributions in the bar are shown in Fig. 4.14b. The observed strain readings are low due to bending in the bar as a result of shear distortion of the beams. The influence of shear distortion is supported by a comparison of the crack patterns and the load versus longitudinal bar strain plots. Figure 4.10 shows the typical shear distortion phenomenon exhibited in the load versus strain plots. The crack patterns for the same test are shown in Fig. 4.5d. The arrows in Fig. 4.5d indicate where the flexural crack became inclined and diagonal tension was apparent. Shear distress appeared at an applied load of 38 kips. Examination of the load versus strain plot (Fig. 4.10) shows that the observed average strain began to deviate from the computed load-strain curve at a load of approximately the same load. Similar correlation was found in all tests exhibiting significant cracking.

Regardless of the strains observed, equilibrium between the internal and external forces at any section in a beam must be satisfied. The internal forces calculated from the average observed bar strains are not in equilibrium with the applied loads on the specimen. Therefore, since the load measurements were considered to be reliable, further discussion involving stress (or strain) in the longitudinal reinforcement will be based on the average strains computed from the applied (measured) load using program PIER, in which the tensile capacity and nonlinearity of the concrete is included. The measured longitudinal strains are used only to identify behavior trends.

4.3.1 Steel Strains Across the Splices. Plots of steel strain (from loads) across the splices can be used to correlate the performance of the splices with observed crack patterns.

Typical strain distributions across the end of the splice at different load levels are shown in Fig. 4.11 for #9 bars (Test 24) and

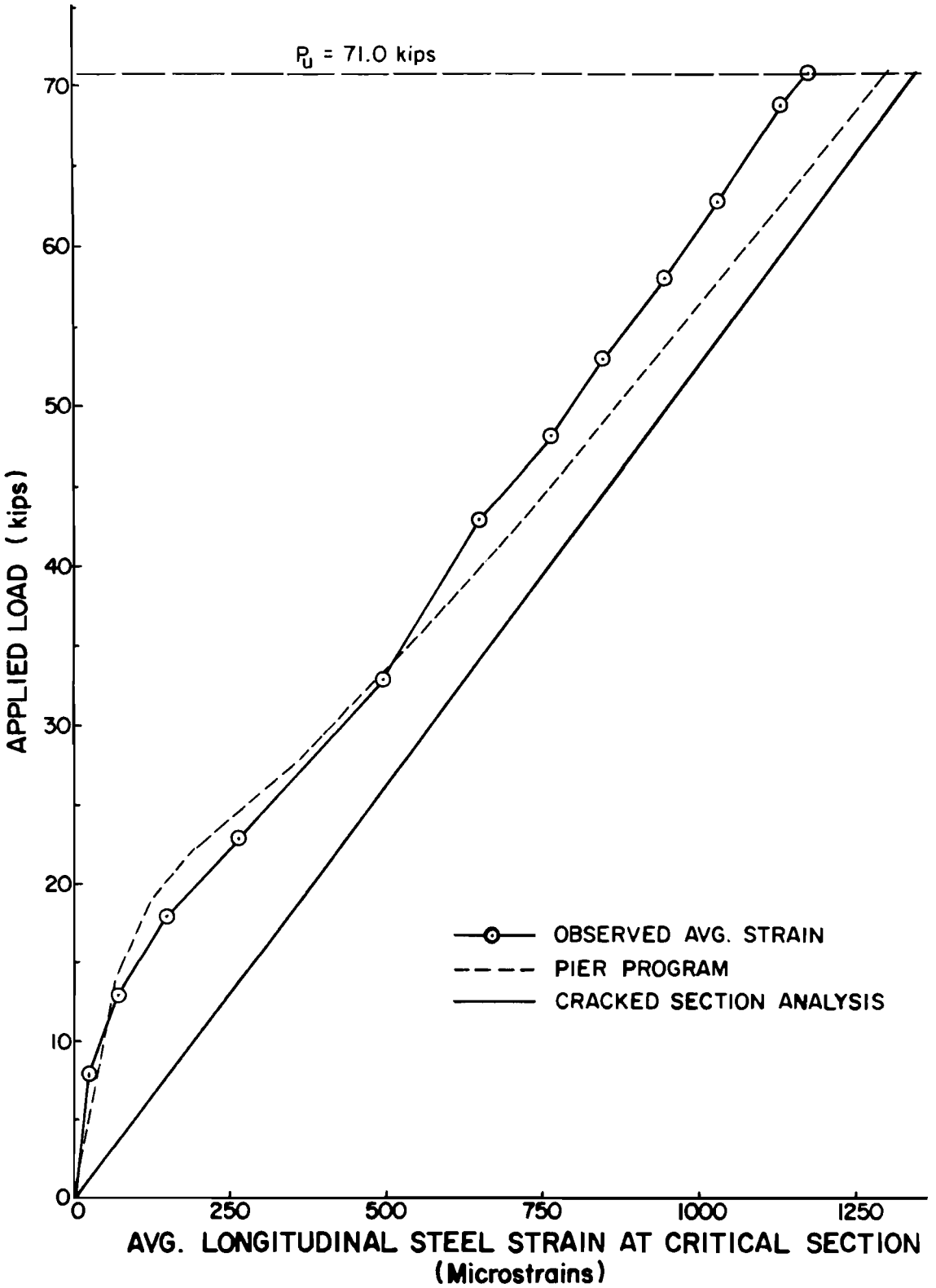

Fig. 4.10 Load vs. strain, Test 20, 40 in. shear span

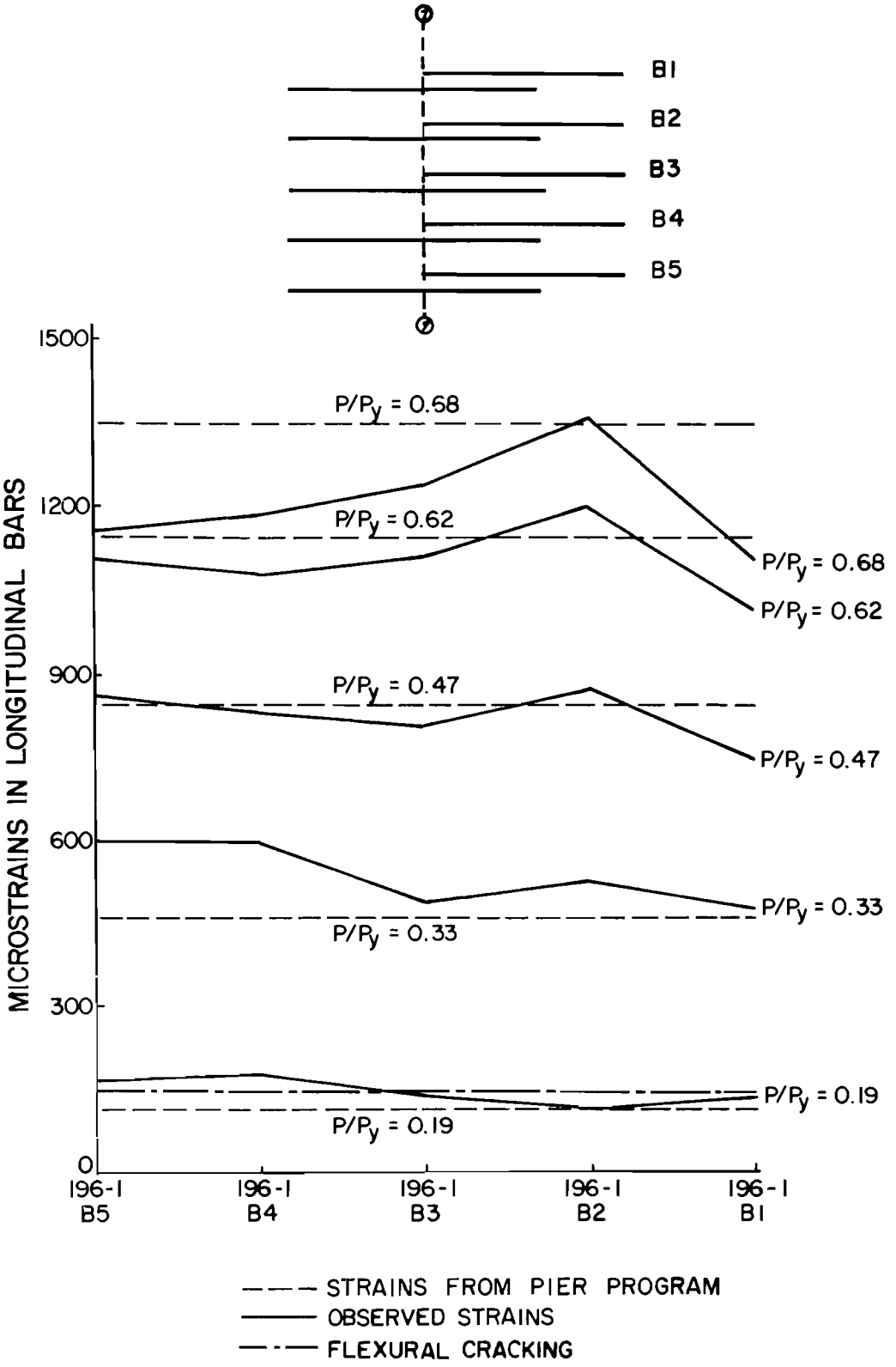

Fig. 4.11 Steel strain distribution across the end of the splice, Test 24

in Fig. 4.12 for #11 bars (Test 11). The dashed lines shown represent the average bar strains as calculated from the loads applied to the beams. Each load level is expressed as a ratio of the applied load to the computed load at which yielding occurs.

The strain distributions at low levels were fairly uniform. At higher loads, the edge bars picked up less strain than the interior bars. This was primarily due to the formation of splitting cracks in the region of the edge bars. The reduced strain in the edge bars was most pronounced in bar B1.

4.3.2 Steel Strains Along the Splice. The distribution of steel strains along selected splices is shown in Figs. 4.13 and 4.14. The rate of change of bar stress (strain) along the splice was proportional to the bond stress developed along the splice length. At low levels of load only a short length of lap near the ends of the splice was required to transfer the stress in the bar to the concrete. The strains at the interior portion of the splice between gage locations 2 and 3 were fairly constant, indicating that very little stress was transferred over the central portion of the splice. As the load increases, the length of lap required to transfer the stress increases. Previous studies [11,13] have shown that as the loads increase, the rate of change of the strain becomes nearly uniform over the entire length of the splice, indicating the development of higher bond stresses along the splice. The strains at sections 1 and 4 are not equal due to the differences in moment at the ends of the splice. The strain distributions shown in Figs. 4.13 and 4.14 are from different splices in the same specimens. In general, the interior splices reach higher strains and corroborate the results shown in Figs. 4.11 and 4.12.

4.3.3 Strains in the Transverse Reinforcement. To understand the behavior of the transverse reinforcement in the splice region, plots of load versus stirrup strain were studied. Figures 4.15 to 4.18 show the typical load strain curves for selected gage locations on the transverse reinforcement.

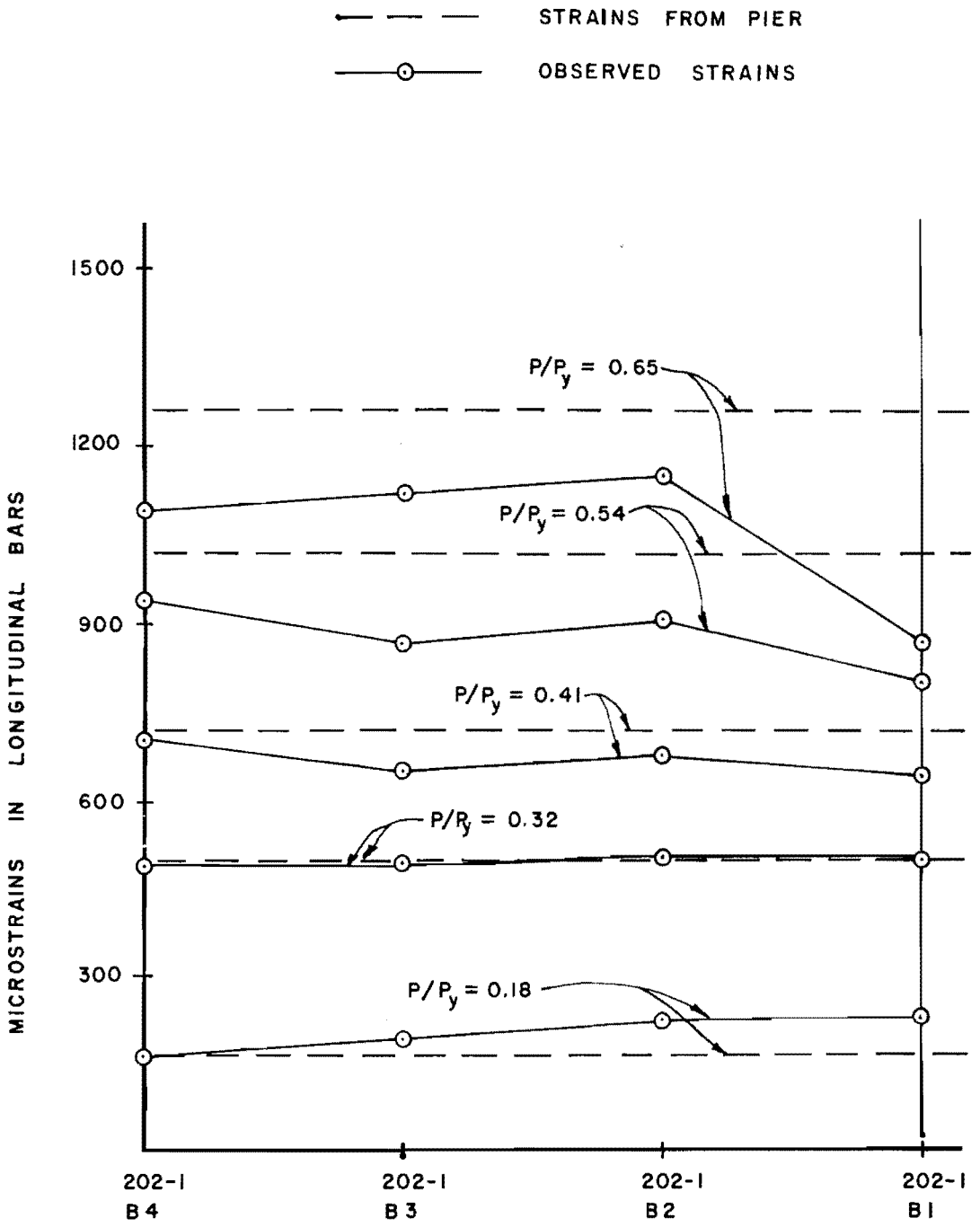

Fig. 4.12 Steel strain distribution across the end of the splice, Test 11

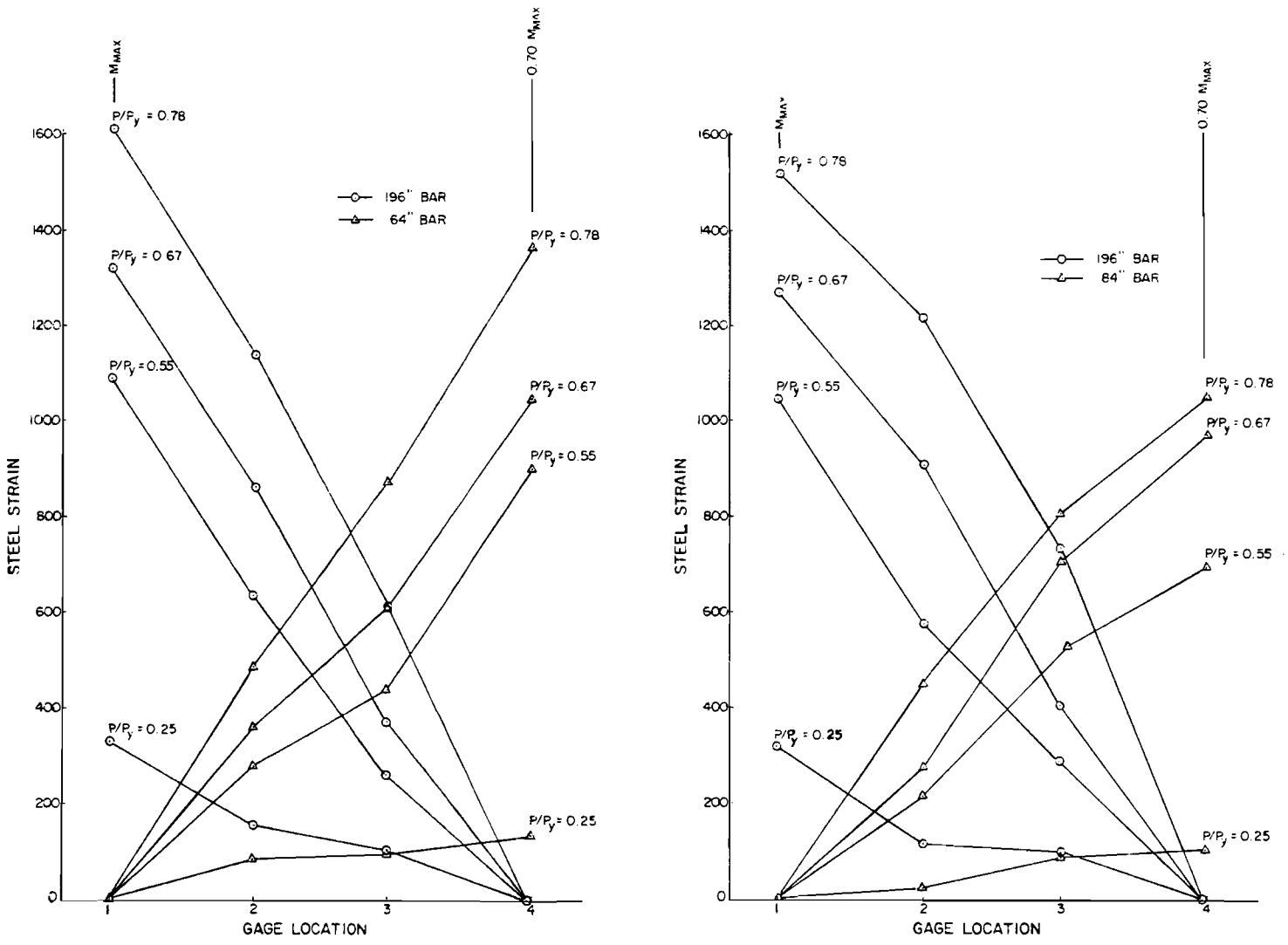

(a) Splice B3--Interior

(b) Splice B1--Exterior

Fig. 4.13 Steel strain history along the splice, Test 22, 53 in. shear span, no transverse reinforcement

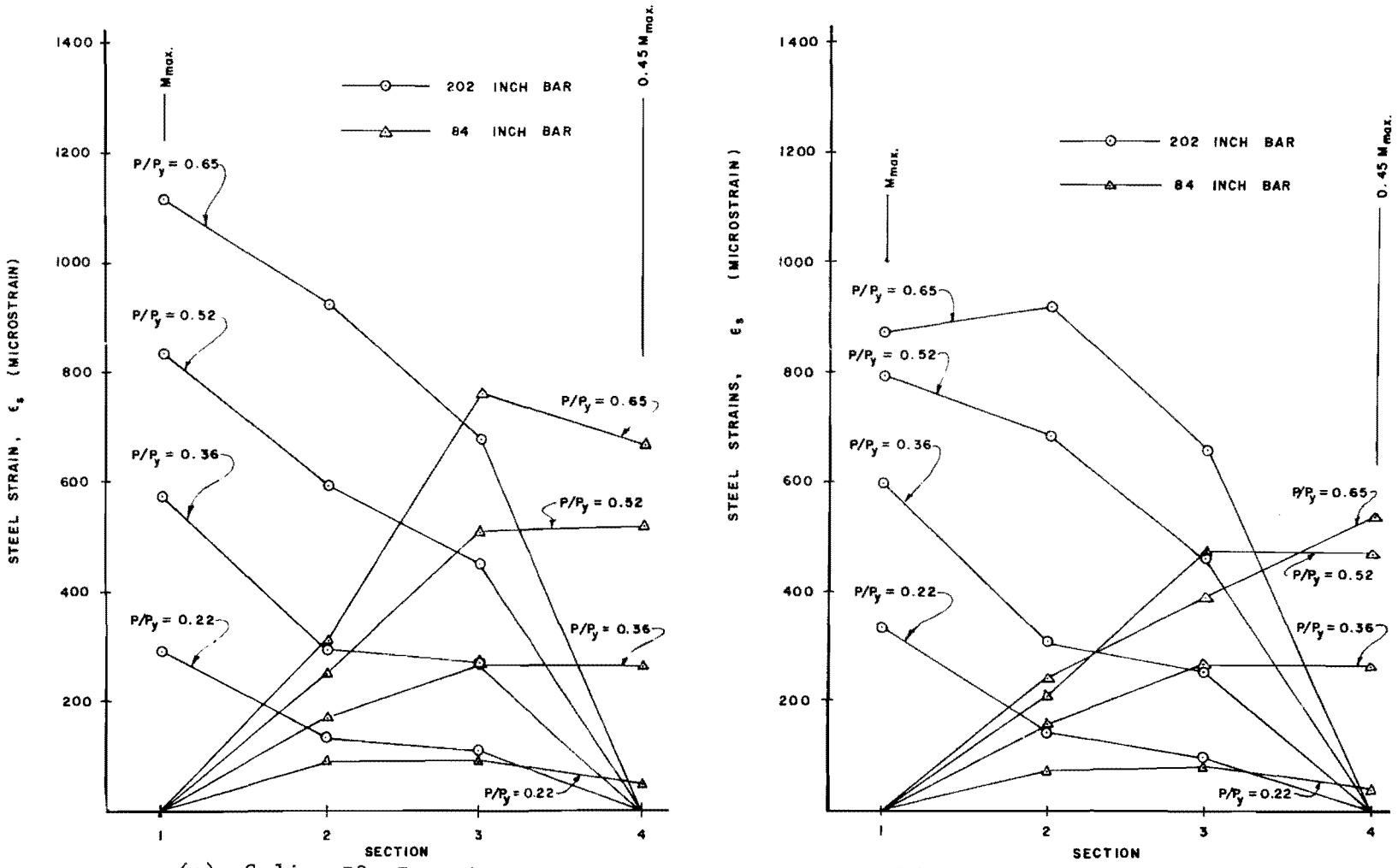

(a) Splice B3--Interior

(b) Splice B1--Exterior

Fig. 4.14 Steel strains along the splice, Test 11, 40 in. shear span, four 6mm @ 5 in.

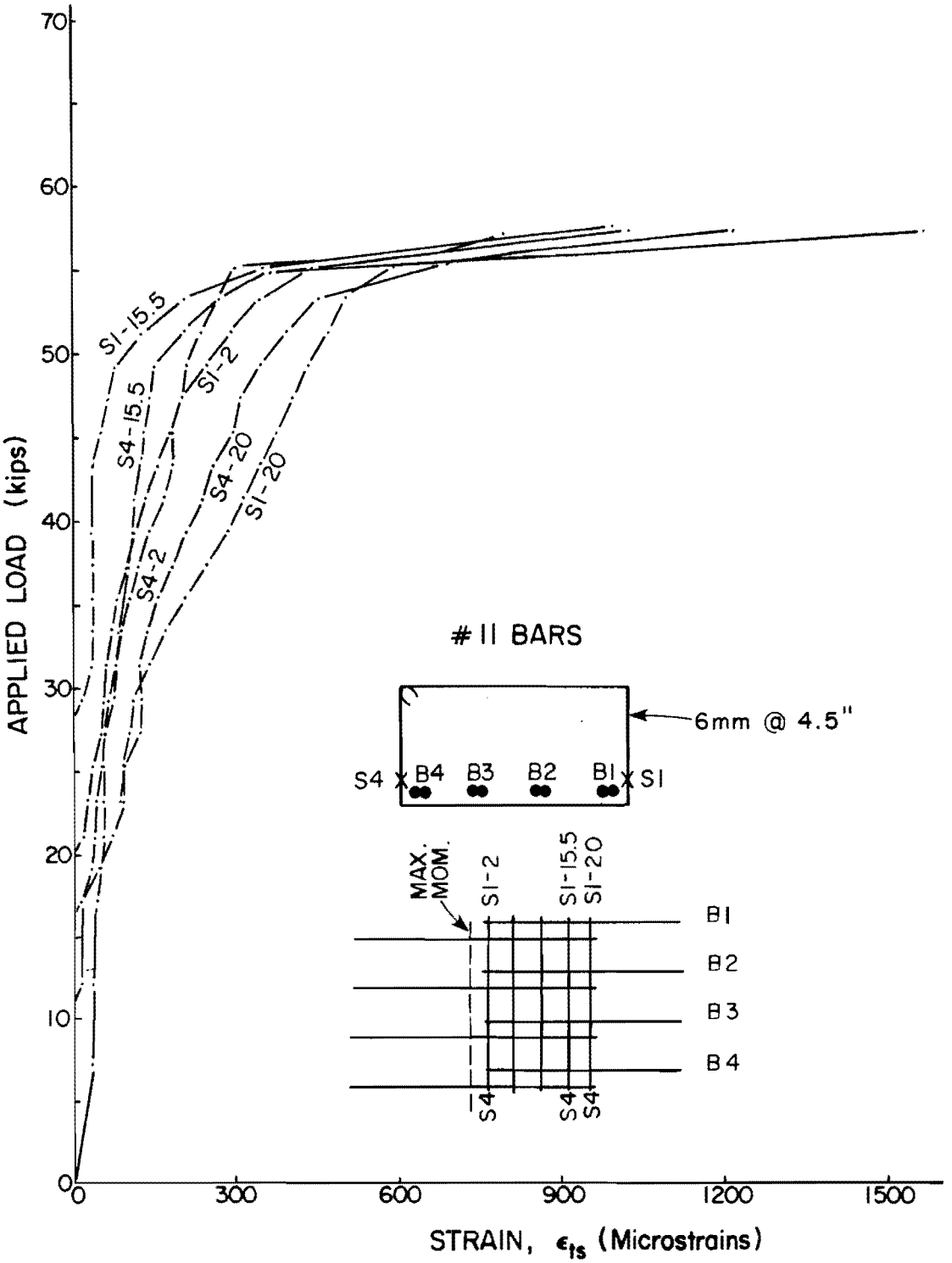

Fig. 4.15 Load vs. strain in stirrups, Test 14, bottom cast, 53 in. shear span

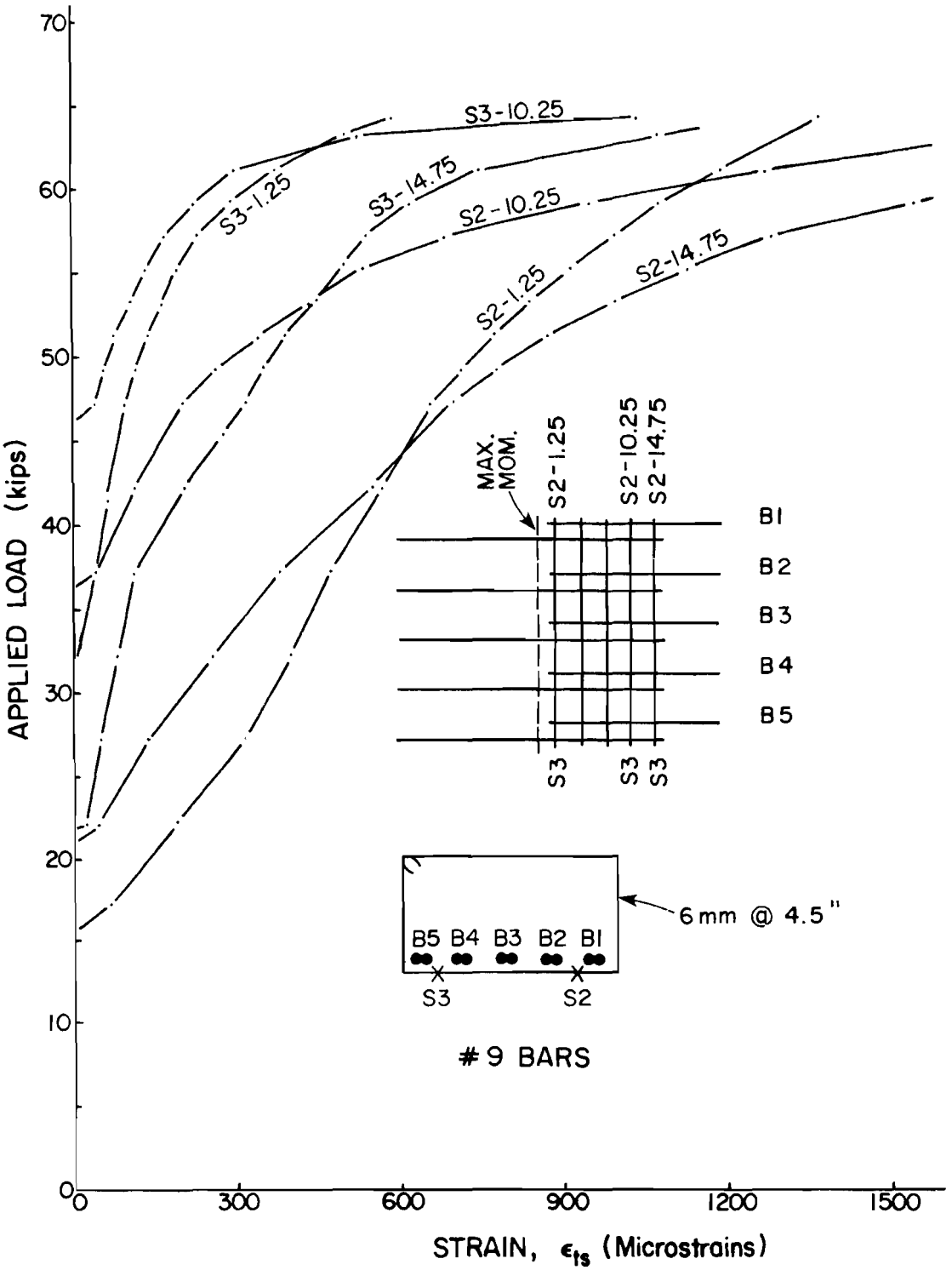

Fig. 4.16 Load vs. strain in stirrups, Test 23, bottom cast, 53 in. shear span

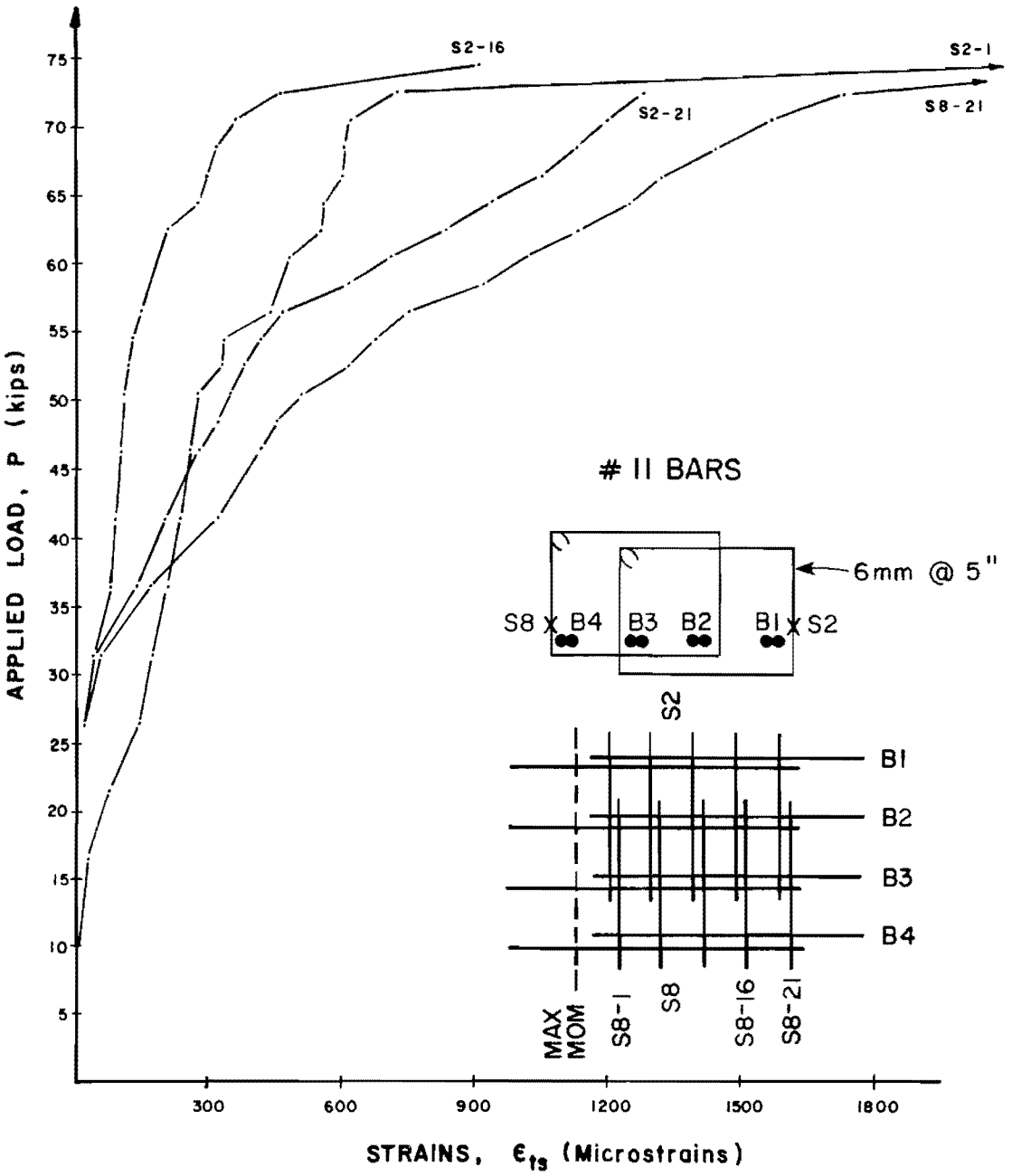

Fig. 4.17 Load vs. strain in stirrups, Test 12, bottom cast, 40 in. shear span

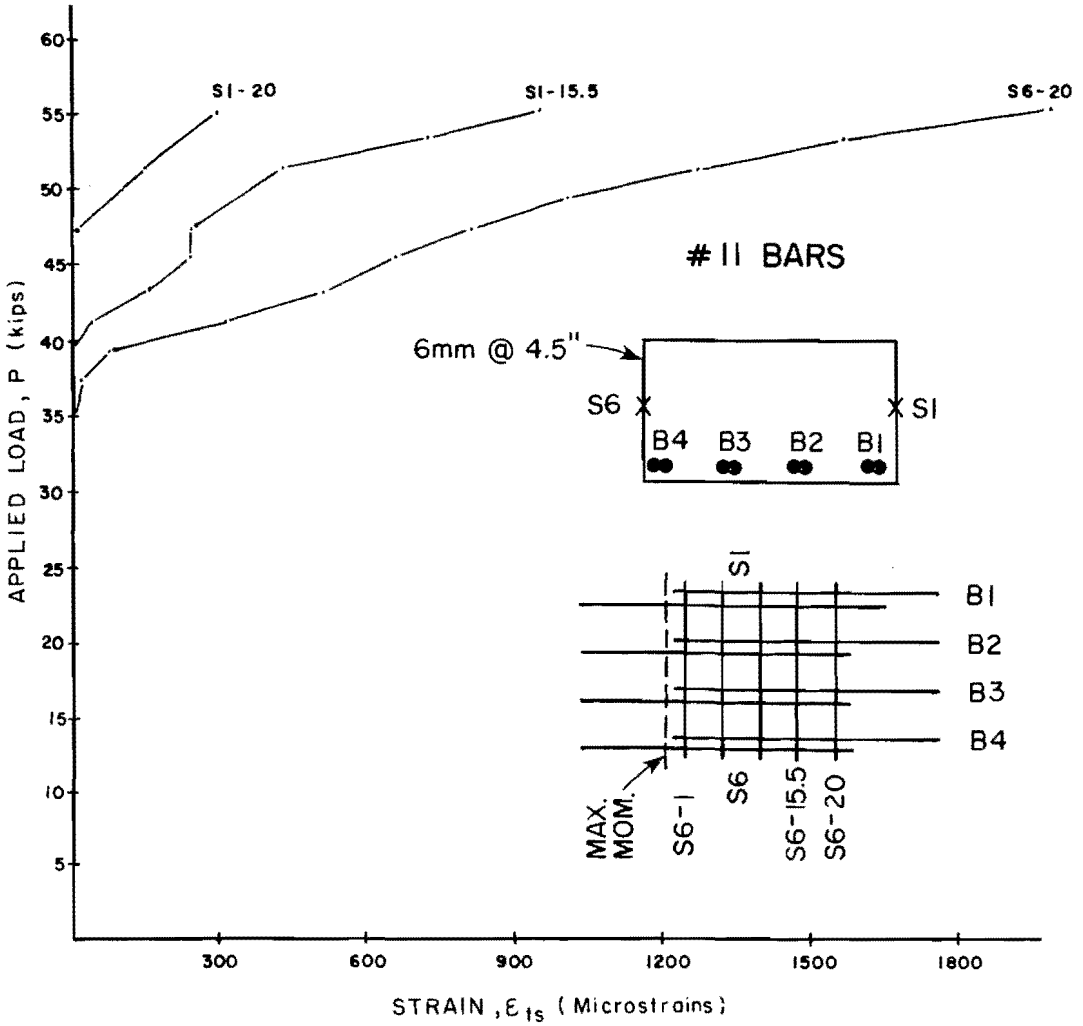

Fig. 4.18 Load vs. strain in stirrups, Test 5, bottom cast, 53 in. shear span

Figure 4.15 shows the load-strain plots for gages S1 and S4 on three instrumented stirrups along a #11 bar splice. These gages give an indication of the effects of side splitting. Examination of the crack patterns indicates that splitting cracks appeared on the surface of the concrete at loads very close to failure. At loads above 55 kips, the stirrup strains increased rapidly.

Figures 4.16 and 4.17 show the strains on the stirrups for two specimens with different transverse steel configurations. Note that the stirrup next to the B1 splice is stressed more rapidly in both cases than it is next to B5 bar. The stirrups closest to the ends of the splice were more effective in resisting splitting distress than were the stirrups near the middle of the splice because the gages on the stirrups closest to the ends always showed the greatest amount of strain.

Figure 4.18 shows the load versus strain plots for gages S1 and S6 at the midheight of the stirrup. Note that the stirrup was not stressed until shear cracking occurred. Initial shear distress in the specimen occurred between loads of 35 to 40 kips as observed from an examination of the crack patterns. In general, there was good correlation between the loads at which shear distress was observed in both the crack patterns and observed strains in the transverse reinforcement.

4.3.4 Strains at Selected Points Around Transverse Reinforcement. By plotting measured strains against gage location on an unfolded stirrup, the strain distributions around the transverse reinforcement may be studied. Figure 4.19 shows typical plots of strains around the transverse reinforcement for the three instrumented stirrups in Test 20. Strains are shown for the highest sustained load and after failure of the splices. The mode of failure and the formation or widening of splitting cracks correlate with the stirrup strain patterns shown in Fig. 4.19. The increase in strain after failure of the splice provides an indication of the extent that the cracks opened up. Figure 4.19b shows that at failure gage S3 was highly strained on the tension face of the beam specimen. Gages S2 and S3 increased more at failure than gages S1 and S4 on the side faces.

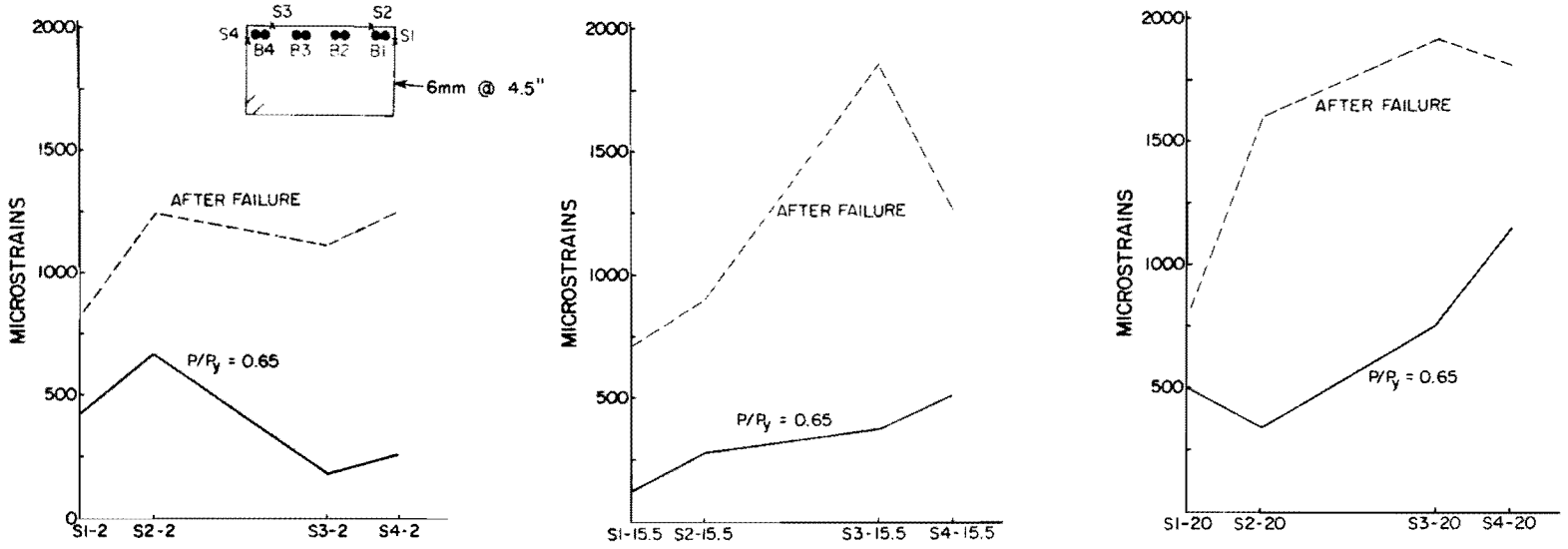

(a) Stirrup 2" from critical section

(b) Stirrup 15.5" from critical section

(c) Stirrup 20" from critical section

Fig. 4.19 Strains around the transverse reinforcement, Test 20, top cast, #11 bars, 40 in. shear span

The mode of failure and locations or widening of splitting cracks can be clearly seen from the strains in Fig. 4.20. Just before failure, gages S3, S8, and S5 showed high strain. The readings indicate that splitting cracks were progressing toward the tension face of both edge bars and were forming on the B4 side face of the specimen. After failure, the gages indicate that the cracks on the tension face at bar B1 and on the side face at bar B4 have opened, while the crack in the tension face at bar B4 opened only slightly. There was a substantial increase in the strain at gage S3 after failure, indicating that splitting cracks on the tension face were extensive along splice B1, as shown in Fig. 4.10.

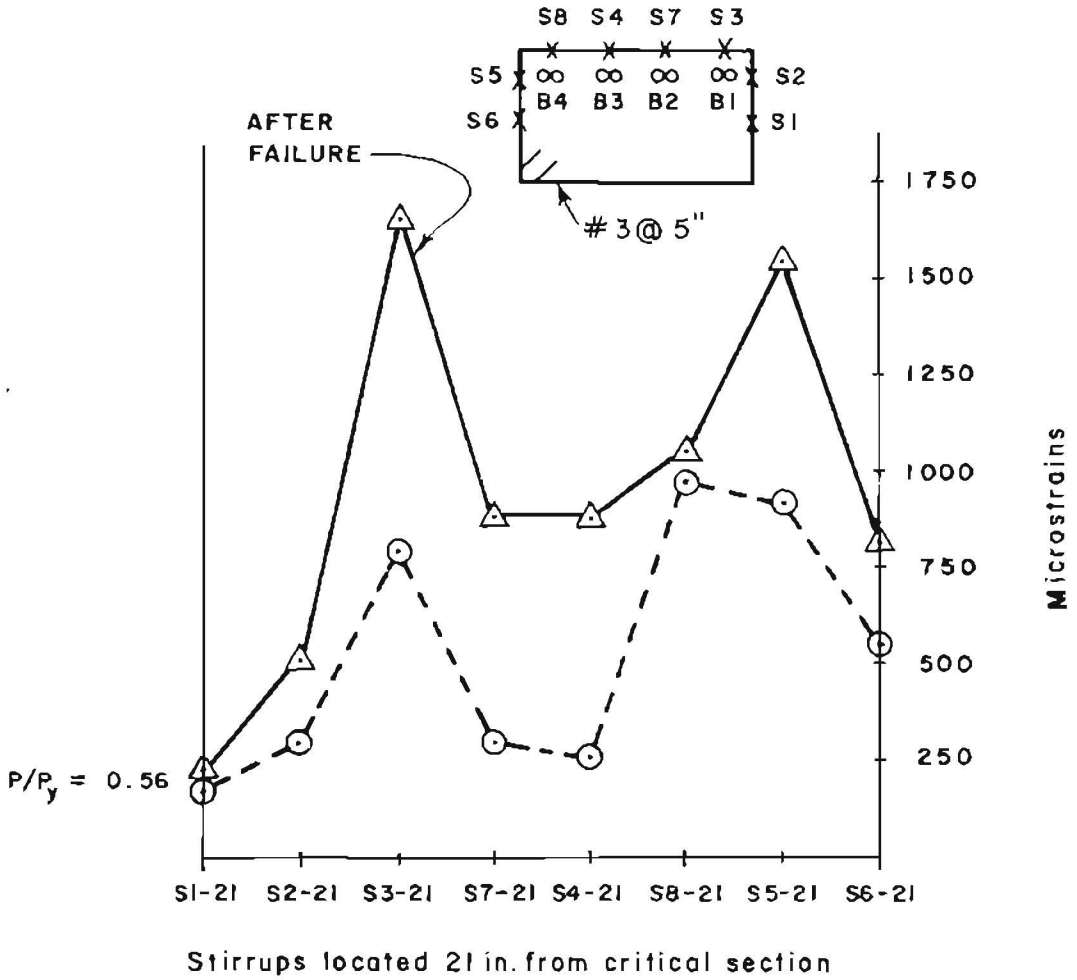

Fig. 4.20 Strains around the transverse reinforcement, Test 1, top cast, #11 bars, 40 in. shear span

CHAPTER 5

EVALUATION OF TEST RESULTS

5.1 Introduction

The results of the splice tests are discussed in this chapter in terms of the main variables: level of shear, amount of transverse reinforcement, configuration of the transverse reinforcement, casting position, and concrete properties. A summary of the test results is shown in Table 5.1. To evaluate the main variables, average bond stresses are compared. Measured bond stresses are calculated using Eq. (2.5). The average steel stress, f_s, was obtained using the PIER program [14] based on the total applied load at failure. The calculated bond stresses are based on the equation developed by Orangun, et al. [1] and are computed using Eq. (2.9).

In order to make comparisons of the results from tests which had different concrete strengths, the average bond stresses were divided by the square root of the concrete compressive strength. This adjustment is reasonable considering that bond stresses are related to concrete tensile strength which is approximately proportional to the square root of the concrete compressive strength. This adjustment has been used by other investigators provided that the variation in concrete strength is not too large. Table 5.1 shows the measured and calculated bond stresses using this adjustment to normalize for concrete strength.

5.2 Level of Shear

Briceno [9] and Krishnaswamy [11] conducted tests in which the splice was in a region of varying moment. Krishnaswamy suggested that the bond stress for a constant moment region be modified (increased) for splices subjected to a moment gradient. However, using the assumption of Tepfers [10] that failure of a splice coincides with the failure of a "cylinder" of concrete surrounding the bar, Orangun, et al. [1] suggested

TABLE 5.1 SUMMARY OF TEST RESULTS

Test	Casting Position	Bar Size	Shear Span a (in.)	Slump (in.)	f_c' (psi)	Measured f_s (ksi)	K_{tr} (Eq. 2.7)	$\frac{u_t}{\sqrt{f_c'}}$ (1) (Eq. 2.5)	$\frac{u_{cal}}{\sqrt{f_c'}}$ (2) (Eq. 2.9)	$\frac{u_t}{u_{cal}}$	$\frac{u_{top}}{u_{bottom}}$ (Observed)
1	T	#11	40	4.5	3700	31.8	0.94	8.37	7.38	1.13	0.89
2	B	#11	40	4.5	3700	35.7	0.94	9.41	9.60	0.98	
3	T	#11	53	4.5	3775	33.9	0.94	8.83	7.38	1.20	0.95
4	B	#11	53	4.5	3775	35.8	0.94	9.33	9.60	0.97	
5	B	#11	53	7.0	4150	39.7	0.43	9.62	9.09	1.06	0.92
6	T	#11	53	7.0	4150	35.6	0.43	8.84	6.99	1.26	
7	T	#11	80	5.5	3825	34.7	0	8.98	6.66	1.35	1.00
8	B	#11	80	5.5	3825	34.8	0	9.01	8.66	1.04	
9	B	#11	80	7.0	4200	39.7	0.43	9.82	9.09	1.08	0.93
10	T	#11	80	7.0	4200	37.0	0.43	9.15	6.99	1.31	
11	T	#11	40	5.5	3825	37.1	0.75	9.61	7.24	1.33	0.94
12	B	#11	40	5.5	3825	39.4	0.75	10.21	9.41	1.09	
13	T	#11	53	3.5	4025	37.0	0.41	9.37	6.98	1.34	0.96
14	B	#11	53	3.5	4025	38.6	0.41	9.77	9.07	1.08	
15	B	#11	53	3.5	4125	41.7	0.41	10.43	9.07	1.15	0.92
16	T	#11	53	3.5	4125	38.6	0.41	9.64	6.98	1.38	
17	T	#11	40	10.5	5425	35.5	0.41	7.73	6.98	1.11	0.82
18	B	#11	40	10.5	5425	43.1	0.41	9.38	9.07	1.03	
19	B	#11	40	6.5	5050	43.7	0.41	9.86	9.07	1.09	0.85
20	T	#11	40	6.5	5050	37.7	0.41	8.42	6.98	1.21	
21	T	#9	53	7.0	5650	39.7	0	9.32	6.70	1.39	0.91
22	B	#9	53	7.0	5650	43.6	0	10.23	8.71	1.17	
23	B	#9	53	7.0	5700	54.2	0.41	12.67	9.12	1.39	0.70
24	T	#9	53	7.0	5700	37.7	0.41	8.81	7.02	1.25	
									Average	1.19	0.90
									Standard Deviation	0.14	0.08

Notes: (1) Includes no transverse reinforcement term.
Calculated directly from measured steel stress

(3) K_{tr} term included.

$u_{cal} = u_c + u_{tr}$, casting position factor = 1.3

that a moment gradient should have little or no effect on the bar stress at failure. It was also concluded that Eq. (2.9) slightly underestimated the strength of splices subjected to a moment gradient, but the difference was not sufficient to revise the basic approach. It should be noted that in the tests studied by Orangun, et al. [1] the splices in the region of variable moment were subjected to a fairly low constant shear force.

The splices tested in this project were in regions of high shear. Four similar pairs of specimens were used to study the effect of the level of shear on the performance of the splice. Each pair of specimens was identical, except for the shear span used to test the specimen. A quantitative comparison of the results in terms of $u_t/\sqrt{f_c'}$ and $(V/bd)/\sqrt{f_c'}$ is shown in Table 5.2. The test results show that the level of shear had an inconsequential effect on the strength of lapped splices. Substantial increases in the level of shear caused negligible changes in the splice strength.

5.3 Transverse Reinforcement

Four pairs of specimens were used to study the effect of the transverse reinforcement on the strength of lapped splices. Comparisons were made of tests with different amounts of transverse reinforcement present in the splice region. Other researchers [1,9,11,13] have found that increased amounts of transverse reinforcement in the splice zone generally improved the performance of the splice.

Table 5.3 shows the comparison of specimens with various amounts of transverse reinforcement in terms of the ratio $u_t/\sqrt{f_c'}$. The comparisons show changes from a decrease of 5 percent to an increase of 24 percent in bond strength with increased amounts of transverse reinforcement.

The maximum increase in calculated bond strength for the splices attributed to the change in transverse reinforcement is only 6 percent. The calculated splice strength is controlled primarily by the lap length and cover or spacing. Although relatively small increases in transverse reinforcement may substantially increase the shear strength of

TABLE 5.2 EFFECT OF LEVEL OF SHEAR ON THE SPLICE STRENGTH

Test No.	Shear Span (in.)	$\frac{u_t}{\sqrt{f_c'}}$	Percent Change	$\frac{V}{\frac{bd}{\sqrt{f_c'}}}$	Percent Increase
3	53	8.83	-5	2.29	22
1	40	8.37		2.80	
4	53	9.33	1	2.39	30
2	40	9.41		3.10	
10	80	9.15	-3	1.53	48
6	53	8.84		2.27	
9	80	9.82	-2	1.63	50
5	53	9.62		2.44	

TABLE 5.3 EFFECT OF THE AMOUNT OF TRANSVERSE REINFORCEMENT ON THE SPLICE STRENGTH

Test	ρ_t (%)	Test $\frac{u_t}{\sqrt{f'_c}}$ (Eq. 2.5)	% Change	Calculated K_{tr} (Eq. 2.7)	Calculated $\frac{u_{cal}}{\sqrt{f'_c}}$* (Eq. 2.9)	% Change
7	0	8.98	+2	0	6.66	+5
10	0.072	9.15		0.33	6.99	
8	0	9.01	+9	0	8.66	+5
9	0.072	9.82		0.43	9.09	
6	0.072	8.84	0	0.33	6.99	+6
3	0.161	8.83		0.72	7.38	
5	0.072	9.62	-3	0.43	9.09	+6
4	0.161	9.33		0.94	9.60	
21	0	9.32	-5	0	6.70	+4
24	0.072	8.81†		0.32	7.02	
22	0	10.23	+24	0	8.71	+3
23	0.072	12.67†		0.41	9.12	
		Ave.	+4.5		Ave.	+5

*Note: A casting position factor of 1.3 has been applied to the top splice calculations

†Superplasticizer (HRWR) added

TABLE 5.4 EFFECT OF THE CONFIGURATION OF TRANSVERSE REINFORCEMENT ON SPLICE STRENGTH

Test No.	Specimen	No. of legs. trans. reinf.	ρ_t (%)	$u_t/\sqrt{f'_c}$	% Increase
1	3-5-40-T	2	0.161	8.37	15
11	2-5-40-7(4)	4	0.129	9.61	
2	3-5-40-B	2	0.161	9.41	9
12	2-5-40-B(4)	4	0.129	10.21	

a section, the change in calculated (and measured) bond strength contributed by the same increase in transverse reinforcement is quite small. However, the inclusion of transverse reinforcement was found to improve the splice performance in terms of control of the size and extent of the splitting cracks. This was particularly true when comparing specimens without transverse reinforcement to specimens with transverse reinforcement.

5.4 Configuration of Transverse Reinforcement

The effect of the configuration of the transverse reinforcement was evaluated by comparing four test specimens, two with 4 legs of transverse reinforcement and two with 2 legs. Table 5.4 summarizes the test results in terms of the ratio $u_t/\sqrt{f_c'}$. The results show an improvement in bond strength for specimens with four legs, even though the ratio of transverse reinforcement was greater for specimens with 2 stirrup legs. Intermediate legs of transverse reinforcement were likely more effective and efficient in improving the performance of lapped splices primarily because each splice was confined by a leg of transverse reinforcement.

5.5 Casting Position

The effect of casting position on the strength of splices was one of the primary variables in the larger research program in which this study is included. Hamad [2] and Luke [3] extensively studied the effect of casting position on both development and splice length.

To study the effects of casting position, 12 beams each containing both a top and bottom splice test zone were tested. Table 5.1 shows the comparisons of the test results in terms of the ratios $u_t/\sqrt{f_c'}$ and u_{top}/u_{bottom} for the effect of casting position. All top splices showed a reduction in bond strength as compared to the bottom splice tests. The casting position factor α which is the reciprocal of u_{top}/u_{bottom} varied from 1.00 to 1.22 except for Specimens 23 and 24 for which the factor was 1.42. The average ratio of top to bottom bond strength was 0.90 with a standard deviation of 0.08.

5.6 Concrete Strength

The results shown in Fig. 5.1 indicate an increase in bond strength with increase in the concrete compressive strength for bottom splices. The assumption that bond stresses vary with the square root of the cylinder concrete strength seems to be reasonable for the bottom splices. For top splices, there is considerable scatter. The measured bond stresses remain almost constant for the relatively small increases in concrete strength. Changes in concrete slump may have influenced top splices more than bottom splices. Tests 17 and 18 are of special interest because superplasticizer was added (noted in Fig. 5.1 with SP). Although the concrete strength was highest in these tests, the bond strength of the top splice (Test 17) was relatively low. More studies are needed to determine the effect of superplasticizers and possible adverse effects of segregation in upper regions of members cast with high fluidity.

5.7 Slump

Since slump can be considered an indication of the amount of concrete sedimentation likely to occur, it was used for comparing top and bottom splice performance. Table 5.5 lists identical specimens except for the concrete slump. For top tests, there is a 6 percent difference in failure load for a change in slump from 3.5 to 7 in. and an 18 percent change for slumps from 3.5 to 10.5 in. For bottom tests, there is no significant variation in bond strength.

It should be noted that there is a variation in the ratio of top to bottom cast splice strength for tests with different slump values. In Table 5.6 it can be seen that for tests with slump of 3.5 in. the ratio was 0.96 and for slumps of 10.5 in. the ratio was 0.84 with ratios for 6.5 and 7.0 in. slump falling between. In general it can be said that the top bars perform more efficiently in concrete with lower slump.

TABLE 5.5 EFFECT OF SLUMP ON BOND STRENGTH

Test No.	Casting Position	Slump (in.)	f'_c (psi)	$P_{ultimate}$ (kips)	$\frac{u_t}{\sqrt{f'_c}}$	$\frac{u_t \text{ (slump)}}{u_t \text{ (3.5" slump)}}$
17	T	10.5	5425	68	7.73	0.82
20	T	6.5	5050	71	8.42	0.89
6	T	7.0	4150	53	8.84	0.94
13	T	3.5	4025	55	9.37	1.00
18	B	10.5	5425	81	9.38	0.96
19	B	6.5	5050	82	9.86	1.01
5	B	7.0	4150	57	9.62	0.98
14	B	3.5	4025	57	9.77	1.00

TABLE 5.6 EFFECT OF SLUMP ON RATIO OF TOP-TO-BOTTOM SPLICE STRENGTH

Test No.	Casting Position	Slump (in.)	f'_c (psi)	$P_{ultimate}$ (kips)	Ratio	$\frac{u_t}{\sqrt{f'_c}}$	% Change
17	T	10.5	5425	68	0.84	7.73	+18
18	B	10.5	5425	81		9.38	
6	T	7.0	4150	53	0.93	8.84	+ 8
5	B	7.0	4150	57		9.62	
20	T	6.5	5050	71	0.86	8.42	+15
19	B	6.5	5050	82		9.86	
13	T	3.5	4025	55	0.96	9.37	+ 4
14	B	3.5	4025	57		9.77	

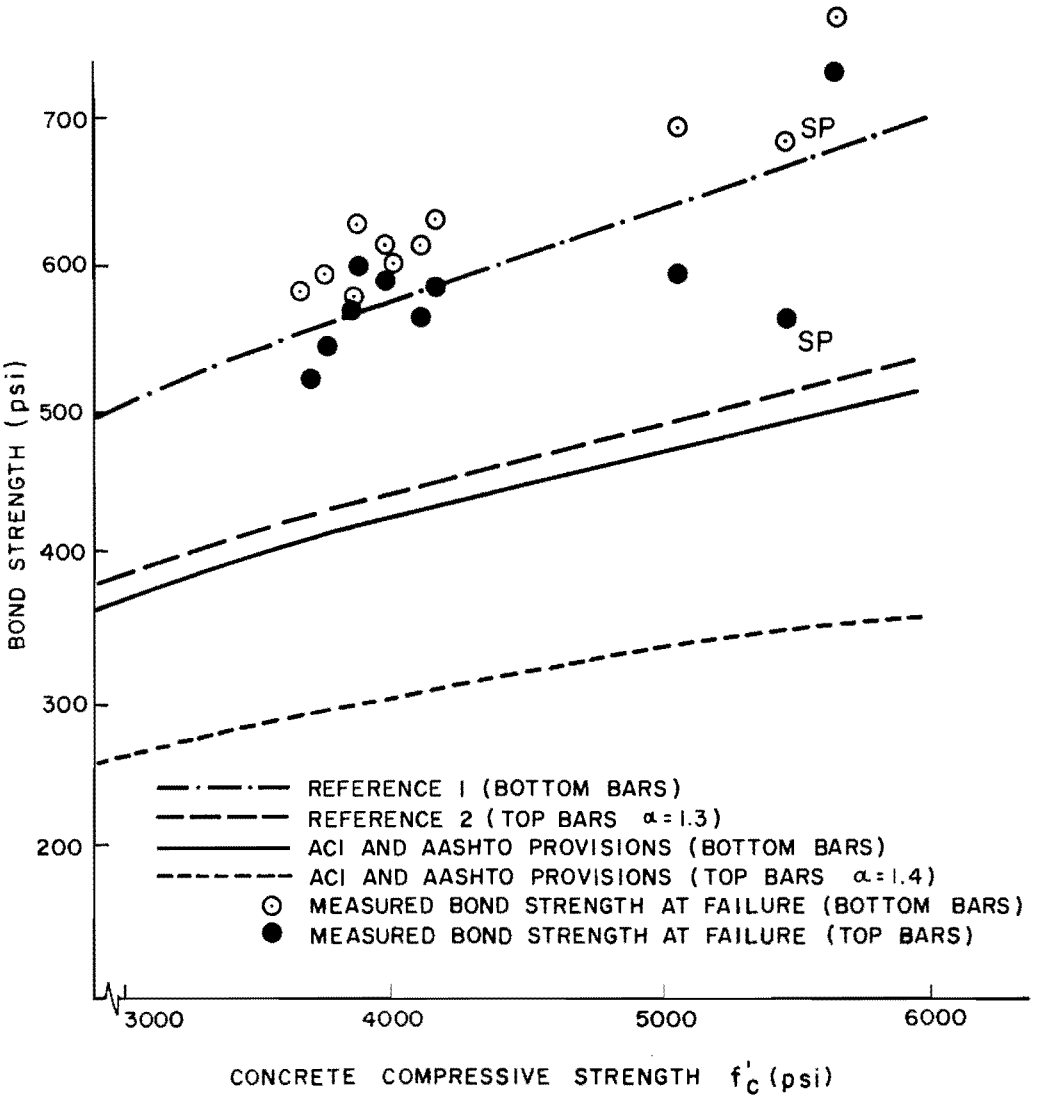

Fig. 5.1 Variation in bond strength with concrete compressive strength

5.8 Splice Location

In all but two tests, one end of the splice began at a section of maximum moment. In all cases a flexural crack appeared at one end of the splice over the support and shear cracks developed as continuations of flexural cracks along the splice. Figure 5.2a shows a freebody diagram of a portion of a beam between two of the cracks. Considering the freebody of the beam segment, the total external transverse force P is resisted by a combination of forces: shear across the compression zone, V_c; dowel force across the flexural crack provided by the flexural reinforcement, V_d; and the vertical components of inclined shearing stresses V_a transmitted across the inclined crack by means of interlocking of the aggregate particles. Bond forces along the bar are transferred to the surrounding concrete and also to the other bar in the splice. Within the concrete, the bond forces generate lateral stresses which produce splitting in the concrete. From the observed crack patterns and splitting, it was felt that the location of the splice in the shear span may influence the response. Therefore, in Tests 15 and 16 the end of the splice was shifted a distance d away from the support (Fig. 3.2).

In order to study the behavior of the top and bottom tests with shifted splices, the results were compared with corresponding top and bottom tests where splices began at the support and the shear spans were 53 and 40 in. with all other variables constant. Figure 5.2b shows the three beam specimens studied and the moment diagram along the beam. Section A is located at the more highly stressed end of the splice and is 40 in. from the load point in all six tests.

Provided that the splice capacity is the same in all beams, the load producing failure should be about equal in the two beams where the end of the splice is located 40 in. from the load point. The load producing failure should be about 33 percent less in the beam where the end of the splice is 53 in. from the load point as compared with the other two beam specimens.

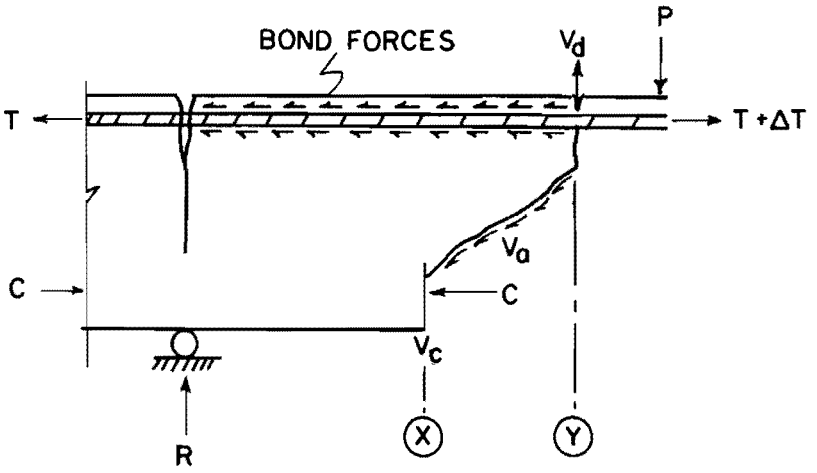

Fig. 5.2a Freebody diagram of concrete block between maximum flexural crack and shear crack

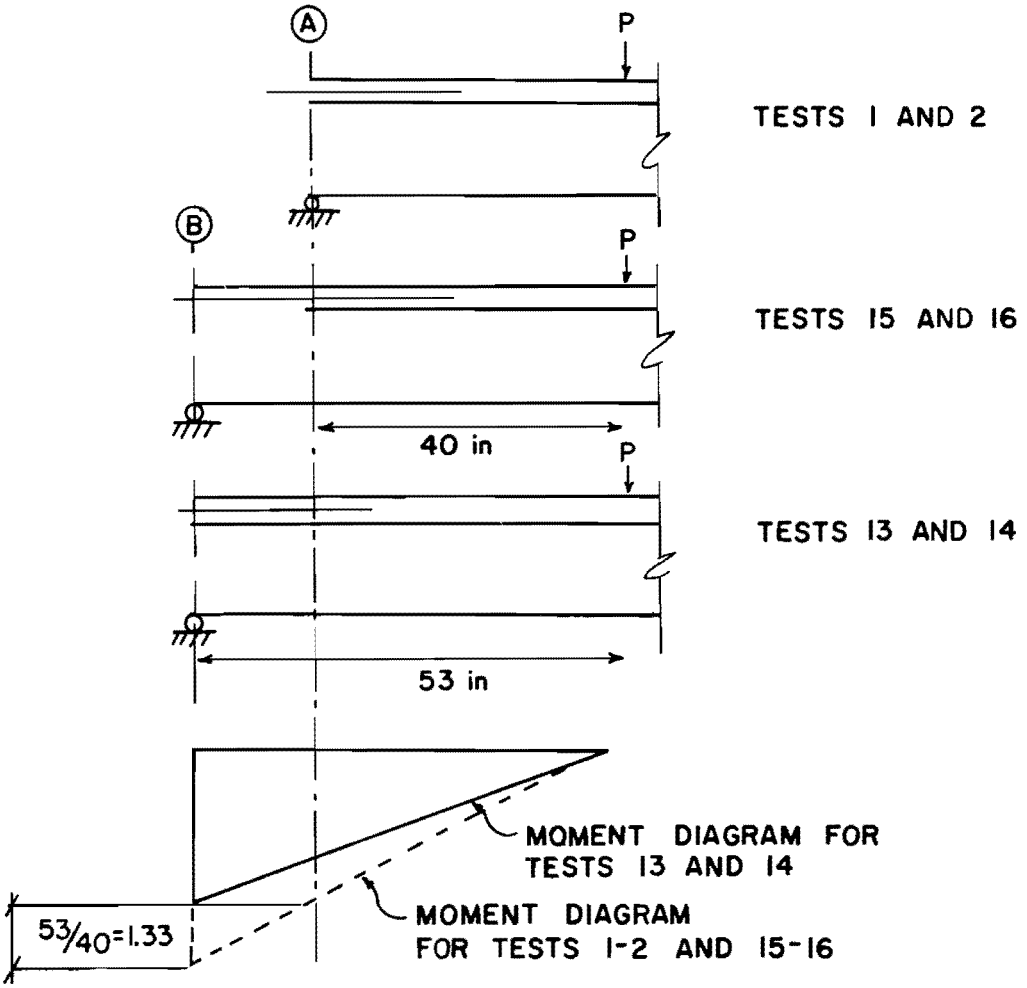

Fig. 5.2b Moment diagram at section A for tests compared

TABLE 5.7 EFFECT OF SPLICE LOCATION ON SPLICE STRENGTH

Test No.	Shear Span	f_c' (psi)	Measured f_s at section A (ksi)	$\frac{P_u}{\sqrt{f_c'}}$ (lbs)
1	40	3700	32	1016
13	53	4025	28	867
16	53*	4125	29	888
2	40	3700	36	1125
14	53	4025	39	902
15	53*	4125	31	954

* shifted

In Table 5.7, Tests 1 and 2 show a 17 and 25 percent increase in normalized load over Tests 13 and 14, which is slightly less than the 33 percent increase expected. On the basis of geometry, Tests 15 and 16 were expected to perform in a manner similar to Tests 1 and 2. However, shifting the splice a distance d from the support did not improve the capacity of the splice and the normalized load was almost identical to that in the beam with splice located at the support (53 in. from the load point). Figure 4.6 shows that cracks in Tests 15 and 16 were shifted to the end of the offset splices where the longitudinal bars are discontinuous. No flexural or shear cracks appeared along the beam between the support and the end of the splice, hence the stress in the steel remained almost constant over the length of the beam from B to A (Fig. 5.1b). Assuming the shear stresses along the crack (V_a in Fig. 5.1a) are negligible, the freebody between X and Y becomes identical to the situation between B and A in the test beam. The freebody shows that the force at Y will be equal to the compressive force at X and bars must develop stresses equal in magnitude to those at the section with a higher moment. Therefore, Tests 15 and 16 behaved in a manner similar to Tests 13 and 14.

CHAPTER 6

SUMMARY AND CONCLUSIONS

6.1 Summary

6.1.1 Test Program. The purpose of this study was to evaluate the influence of shear on the strength of lapped splices. Twenty-four tests were conducted to investigate the effects of level of shear, amount and configuration of transverse reinforcement, casting position, and concrete properties on the performance of the splice. The specimens consisted of simply supported beams with both ends cantilivered over the supports. The splices were subjected to a moment gradient and high shear. The specimens were designed so that a bond failure would occur in the specimen before the stress in the steel reached yield or the section failed in shear. The crack patterns at failure and steel strain distributions were used to describe the behavior of the specimens.

6.1.2 Variables. The main variables in this study were as follows:

(a) Level of Shear. Three different shear spans, 40 in., 53 in., and 80 in., were used to vary the level of shear. With an effective depth of 13.3 in., the a/d ratios were 3.0, 4.0, and 6.0, respectively.

(b) Transverse Reinforcement. Three levels of transverse reinforcement were used in the test specimens: (1) no transverse reinforcement, (2) the area of steel providing the ACI 318-77 and AASHTO minimum requirements (shear strength contributed by transverse reinforcement), and (3) the area providing twice the code minimum. Shear on some specimens exceeded the shear capacity of the concrete section. Therefore, the transverse reinforcement was required to carry shear and to resist splitting along the splice.

(c) Configuration of Transverse Reinforcement. Approximately the same area of transverse reinforcement was provided by using two different configurations--two #3 legs @ 5 in. and four 6mm legs @ 5 in.

(d) Casting Position. Each beam specimen contained both a top cast and a bottom cast splice region. The top splices had 12.6 in. of concrete cast below the bar, thereby classifying the splices as top reinforcement by the ACI and AASHTO codes.

(e) Concrete Properties. Concrete strength and slump were varied. Concrete strength for beam specimens with #11 longitudinal bars ranged from 4025 psi to 5425 psi. Concrete strength for tests with #9 longitudinal bars was 5700 psi. The slump varied from a low of 3.5 in. to a high of 10.5 in. The 10.5 in. slump was obtained by adding a superplasticizer (HRWR) in powder form to the mix before casting.

(f) Bar Size. Two different bar sizes were used. Twenty tests contained #11 longitudinal bars, and four contained #9 longitudinal bars. All were designed to develop about the same bond strength.

(g) Splice Location. In two tests the splice was shifted a distance d (13.3 in.) away from the support and the results compared with tests where one end of the splice started at the section where maximum moment was developed, i.e. right at the support of the overhanging part of the beam.

6.1.3 Specimen Behavior. All of the specimens exhibited a main face and side face splitting failure. Initial splitting cracks developed in the main cover over the edge splice. As splitting cracks developed on the sides of the specimen, the corner edge "block" tended to break loose, destroying the bond on the edge splice and causing the main cover over the interior splices to split and lift off.

The behavior of the specimens was categorized according to shear span. The specimens with a 40 in. shear span were subjected to the highest levels of shear and exhibited the greatest amount of shear distress. The crack patterns were dominated by diagonal tension cracks. The specimens with a 53 in. shear span showed both flexural and shear cracking. Flexural cracks extended approximately to mid-depth of the beam with diagonal tension cracks propagating from the flexural cracks at approximately two-thirds of ultimate. The specimens with an 80 in. shear span had the lowest level of shear and showed primarily flexural cracking. Inclined shear cracks formed only at ultimate and propagated from the flexure cracks.

6.2 Conclusions

6.2.1 Effect of Test Variables. Based on the results from the specimens tested in this study, the following observations and conclusions were made:

(1) Level of Shear. The level of shear had an inconsequential effect on the strength of lapped splices. With substantial increases in the level of shear, only negligible changes in the bond strength were observed.

(2) Transverse Reinforcement. Transverse reinforcement was found to be effective in resisting splitting produced by anchorage distress in addition to its traditional role as primary reinforcement for the diagonal tension produced by shear stresses on the section. Therefore, the transverse reinforcement is fully effective in carrying shear and in resisting splitting along the splice. The entire area of transverse reinforcement can be considered in calculating shear capacity and splice length (Eq. 2.11). Inclusion of transverse reinforcement was found to substantially improve the performance. With transverse reinforcement, the splitting distress was less severe and greater deflections prior to failure were observed. The increases in calculated bond strength attributed to the transverse reinforcement were small, even though the transverse reinforcement substantially increased the calculated shear strength of the section.

(3) Configuration of Transverse Reinforcement. The use of intermediate tie legs at each splice to provide the required area of transverse reinforcement improved the splice strength as compared to using only two legs as in a single perimeter hoop.

(4) Casting Position. The test results showed a decrease in splice strength for top splices with Z = 13.3 in. Top splices had average strengths of 90 percent (with a standard deviation of about 8 percent) of the bottom splice strength.

(5) Concrete Slump. Top splices performed more efficiently in concrete with lower slumps than in high slump concrete. Further research is urgently needed to evaluate the influence of high slump concrete produced with the use of additives on the bond strengths of top reinforcement.

(6) Splice Location. Shifting the splice a distance d away from the section of maximum moment did not improve the capacity of the splice. The load sustained was about the same as if the splice had been located at the critical section (maximum moment).

The tests performed in this study were subjected to severe conditions with regard to splice strength. Placing one end of the splice at the point of maximum moment, subjecting the splice to high levels of shear, and casting concrete with high slumps and relatively low concrete strengths are situations not routinely encountered in design or recommended as good design practice. Nevertheless, the splices performed quite well and provide data for evaluation of code provisions and formulation of recommendations for design which are not excessively conservative.

REFERENCES

1. Orangun, C. O., Jirsa, J. O., and Breen, J. E., "The Strength of Anchored Bars: A Reevaluation of Test Data on Development Length and Splices," Research Report 154-3F, Center for Highway Research, The University of Texas at Austin, January 1975.

2. Hamad, Bilal S., "Effect of Casting Position on Development of Anchored Reinforcement," Unpublished Master's Thesis, The University of Texas at Austin, May 1979.

3. Luke, Joseph John, "The Effect of Casting Position on Development and Lapped Splice Length Requirements for Deformed Reinforcement," Unpublished Master's Thesis, The University of Texas at Austin, December, 1979.

4. Luke, J. J., Hamad, B. S., Jirsa, J. O., and Breen, J. E., "The Influence of Casting Position on Development and Splice Length of Reinforcing Bars," Research Report 242-1, Center for Transportation Research, The University of Texas at Austin, August 1980.

5. Warren, George E., "Anchorage Strength of Tensile Steel in Reinforced Concrete Beams," Unpublished Ph.D. Dissertation, Iowa State University of Science and Technology, Ames, Iowa, 1969.

6. Building Code Requirements for Reinforced Concrete (ACI 318-77), American Concrete Institute, Detroit, 1977.

7. ACI Committee 408, "Rationale for Suggested Development, Splice, and Standard Hook Provisions for Deformed Bars in Tension," Concrete International, Proc. V. 1, No. 7, July 1979.

8. AASHTO Subcommittee on Bridges and Structures, Interim Specifications, Bridges, 1979, American Association of State Highway and Transportation Officials, Washington, D.C., 1979.

9. Ferguson, P. M. and Briceno, Eduardo A., "Tensile Lap Splices Part I: Retaining Wall Type, Varying Moment Zone," Research Report 113-2, Center for Highway Research, The University of Texas at Austin, July 1969.

10. Tepfers, R., "A Theory of Bond Applied to Overlapped Tensile Reinforcement Splices for Deformed Bars," Publication 73:2, Division of Concrete Structures, Chalmers University of Technology, Goteborg, Sweden, 1973.

11. Krishnaswamy, C. N., "Tensile Lap Splices in Reinforced Concrete," Unpublished Ph.D. Dissertation, The University of Texas at Austin, December 1970.

12. Chinn, J., Ferguson, P. M., and Thompson, J. N., "Lapped Splices in Reinforced Concrete Beams," Journal of the American Concrete Institute, Proc. V. 52, October 1955.

13. Thompson, Mark A., Jirsa, J. O., Breen, J. E., and Meinheit, Donald F., "The Behavior of Multiple Lap Splices in Wide Sections," Research Report 154-1, Center for Highway Research, The University of Texas at Austin, January 1975.

14. Poston, Randall W., "Computer Analysis of Slender Nonprismatic or Hollow Bridge Piers," Unpublished Master's Thesis, The University of Texas at Austin, May 1980.

15. Zekany, Andrew John, "Effect of Shear on the Strength of Lapped Splices," Unpublished Master's Thesis, The University of Texas at Austin, April 1980.

16. Neumann-Ladenzon, Simon, "Influence of Concrete Properties in the Behavior of Deformed Bar Splices Subjected to Moment Gradients," Unpublished Master's Thesis, The University of Texas at Austin, August 1980.